Annales Societatis Geologorum Poloniae (2016), vol. 86: 355–377. doi: https://doi.org/10.14241/asgp.2016.008

PRESSURE DISSOLUTION FEATURES IN OXFORDIAN MICROBIAL-SPONGE BUILDUPS WITH PSEUDONODULAR TEXTURE, KRAKÓW UPLAND, POLAND

Jacek MATYSZKIEWICZ & Alicja KOCHMAN

AGH University of Science and Technology, Faculty of Geology, Geophysics and Environment Protection, al. Mickiewicza 30; 30-059 Kraków, Poland; e-mails: jamat@geol.agh.edu.pl; kochman@geol.agh.edu.pl

Matyszkiewicz, J. & Kochman, A., 2016. Pressure dissolution features in Oxfordian microbial-sponge buildups with pseudonodular texture, Kraków Upland, Poland. *Annales Societatis Geologorum Poloniae*, 86: 355–377.

Abstract: Part of the Oxfordian carbonate buildups in the southern part of the Kraków Upland is developed as pseudonodular limestones, which represent segment reefs. These limestones are composed of connected, rounded-oval to subangular carbonate pseudonodules. The pseudonodules, densely packed within the limestone, fall out easily under mechanical stress.

The recently observed texture of pseudonodular limestones resulted from two stages of chemical compaction. During the first stage, in the Late Jurassic, high-amplitude and low-amplitude stylolites and dissolution seams were formed. The sites particularly favourable for the development of high-amplitude stylolites were the boundaries between already lithified fragments of the laminar, rigid microbial-sponge framework. The low-amplitude stylolites formed mainly in the intercalated wackestone-packstone, which was lithified somewhat later; hence, the dissolution seams originated at the contacts between the rigid microbial-sponge framework and the wackestone-packstone.

After Early Cretaceous erosion, which decreased the burial load, Late Cretaceous sedimentation enabled the renewal of pressure dissolution. Thus, some low-amplitude stylolites evolved into dissolution seams. In stylolites composed of both low- and high-amplitude segments, dissolution proceeded at the bases of interpenetrating high-amplitude stylolite columns, with the simultaneous transformation of low-amplitude stylolite segments into dissolution seams. These seams, which formed at the initial stage of chemical compaction, were subjected in turn to further pressure dissolution, giving rise to the formation of horsetail structures.

The vertical stress field, which triggered the pressure dissolution processes, presumably resulted in the formation of high-angle and vertical incipient tension gashes. At the beginning of the processes, these gashes remained closed. In the Cenozoic, under the extensional regime generated by overthrusting Carpathian flysch nappes, some high-angle and vertical dissolution seams and low-amplitude stylolites opened up, forming deformed dissolution seams and deformed stylolites. Under the same conditions, the high-angle and vertical tension gashes opened up as well.

Subsequently, during the exposure period, unloading fractures developed, partly as a result of the opening of some subhorizontal and horizontal dissolution seams and stylolites. The unloading fractures, along with the already existing vertical and high-angle tension gashes, formed the network changing the limestone into pseudonodules of various shapes and sizes. The open spaces between the limestone fragments became local conduits for karst waters.

Key words: Pressure dissolution features, pseudonodularity, microbial-sponge buildups, Oxfordian, southern Poland.

Manuscript received 9 December 2015, accepted 16 May 2016

INTRODUCTION

Pseudonodular limestone is defined as a rock composed of densely packed, connected rounded-oval to subangular carbonate nodules (e.g., Hummel, 1960; Clari *et al.*, 1984; Dromart, 1989; Matyszkiewicz, 1994, 1997; Martire, 1996; Clari and Martire, 1996; Marok and Reolid, 2012). The boundaries between nodules are indistinct. The nodules are densely packed within the limestone, falling out easily under mechanically induced stress.

Pseudonodular (Polish: *zrostkowe*) limestones are a peculiar facies of the Upper Jurassic carbonates, common in the southern part of the Kraków Upland, in the Mników area (Fig. 1). Spectacular exposures of pseudonodular limesto-

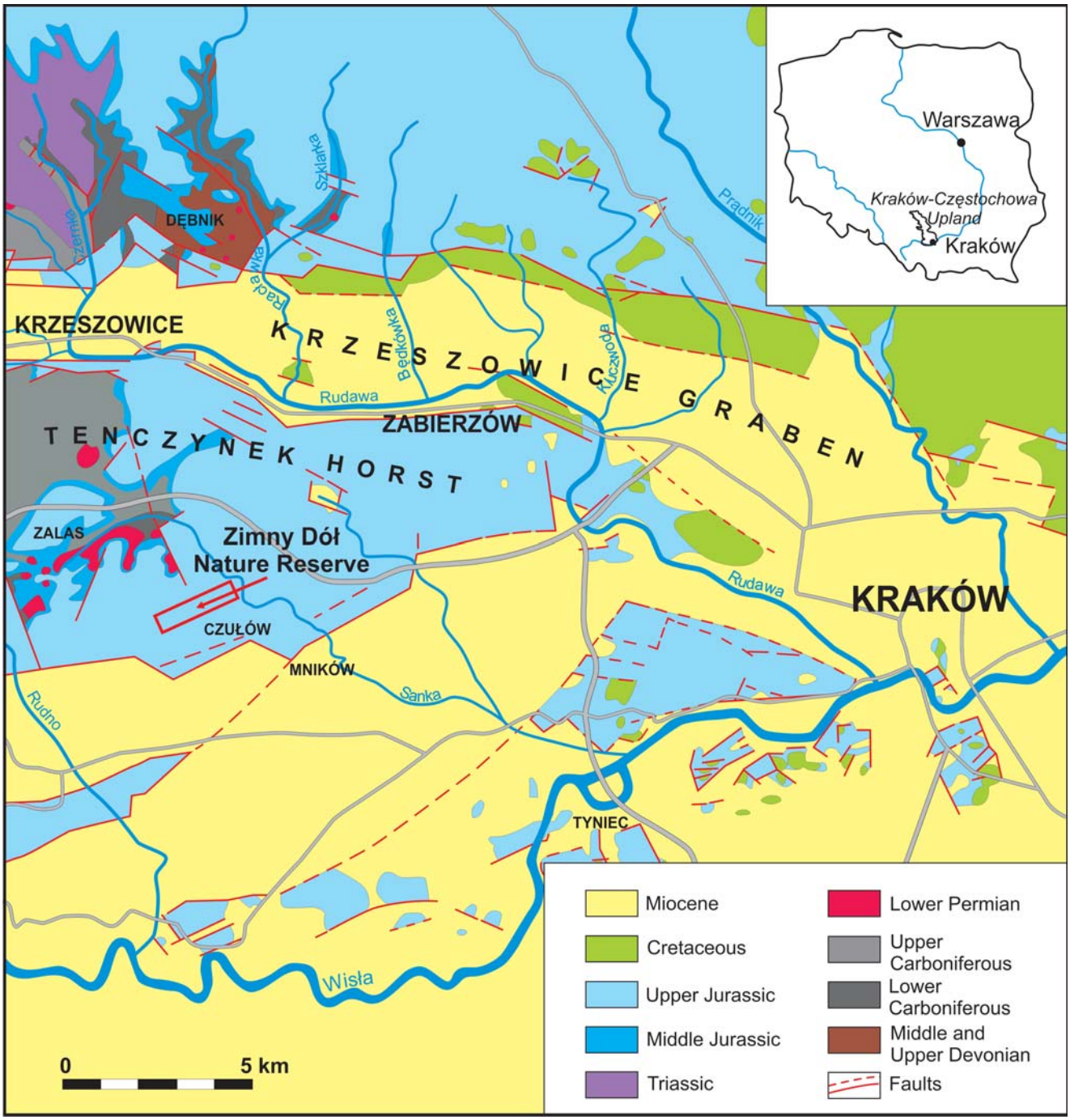

Fig. 1. Location of the Zimny Dół Nature Reserve superimposed on a geologic bedrock map after Gradziński (2009).

nes are known from the Zimny Dół Valley, near the village of Czułów (Fig. 2). In 1991, thanks to the efforts of Professor Ryszard Gradziński, an abiotic nature reserve was established there.

The origin of the pseudonodular limestones of the Zimny Dół Valley was discussed by Dżułyński (1952) and Matyszkiewicz (1994, 1997) and also noted by Gradziński (1972), Gradziński and Baryła (1986, 2005), and Gradziński and Musielewicz-Jasińska (1992).

The pseudonodular limestones of the Mników area were described for the first time by Dżułyński (1952), who interpreted their origin as resulting from the combined effects of bottom currents and later diagenetic transformations. In his interpretations, the currents removed some of the unlithified carbonate mud and supplied larger fossils, mostly small ammonites, siliceous sponges and brachiopods. After deposition, diagenetic processes caused the redistribution of calcium carbonate, which accumulated around the fossils and formed concretions, enveloped in the sediment that was richer in clay.

Matyszkiewicz (1994, 1997) excluded the action of bottom currents; as the formative process of the pseudonodular limestones, he proposed chemical compaction, affecting the inhomogeneous sediment, composed mostly of mi-

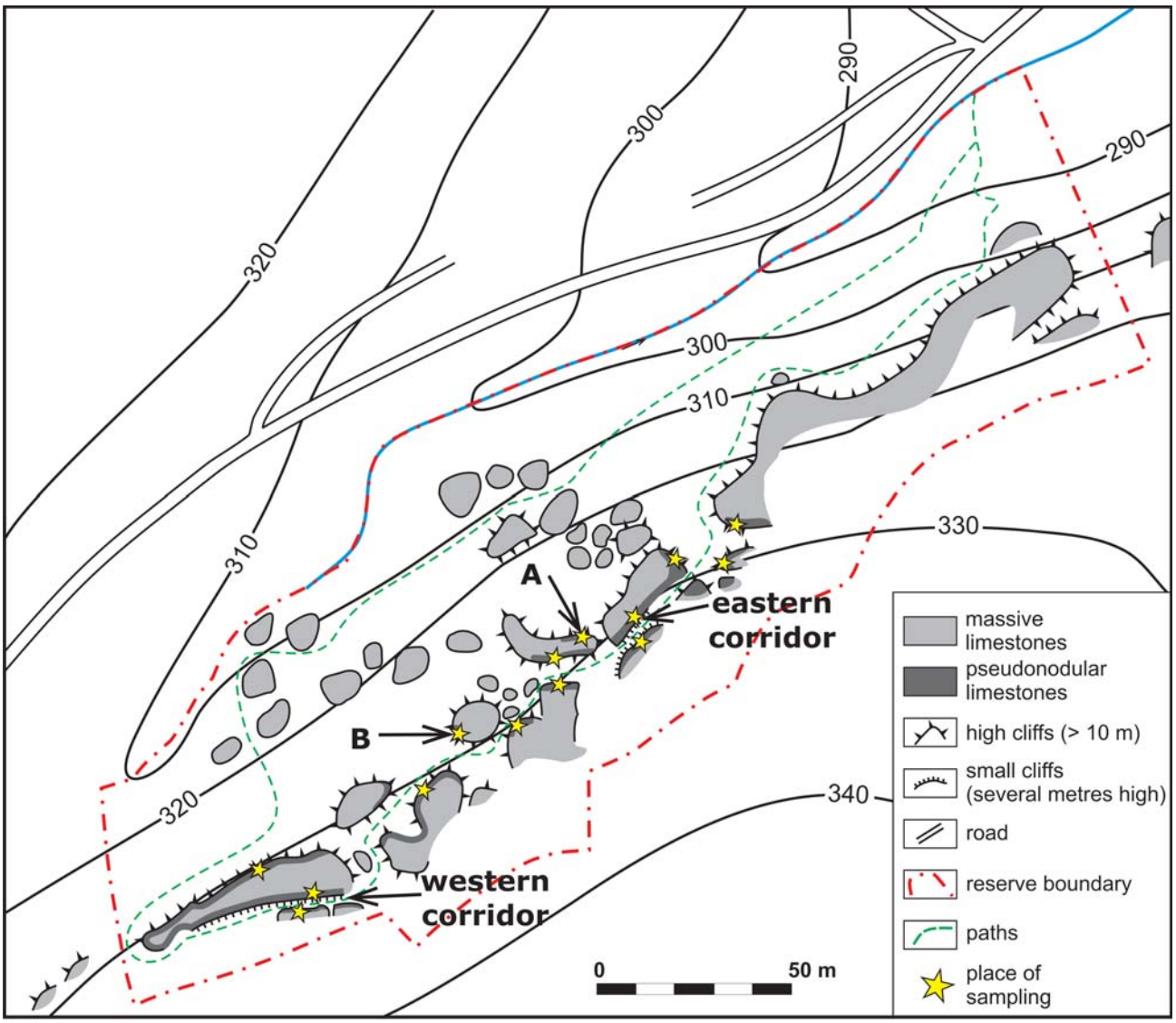

Fig. 2. Sketch of Upper Jurassic tors in the Zimny Dół Nature Reserve (after Gradziński and Baryła, 2005) with location of pseudonodular limestones exposures. Points marked as A, B, and eastern and western corridors are outcrops described in detail.

crobialites and calcified siliceous sponges, in which an initial, laminar rigid framework had developed (cf. Pratt, 1982). Furthermore, the principal role in the formation of the pseudonodular limestones was played by pressure dissolution processes, which generated numerous pressure dissolution features (PDFs), separating the pseudonodules. During later diagenetic stages, some PDFs were transformed owing to the combined action of solutions circulating within the rock formation, karstification, and other weathering processes.

The paper below presents the development of pressure dissolution features (PDFs) along with a detailed reconstruction of the processes, which led to the formation of recently observed textures of the pseudonodular limestones.

AREA OF STUDY

The Kraków Upland is located in the area of the Silesian–Kraków Homocline. Its southern part is cut by numerous tectonic horsts and grabens (Fig. 1), resulting mostly from an extension regime generated in the Cenozoic by overthrusting Carpathian nappes, although their formation already had been initiated in the Late Jurassic or even earlier (Matyszkiewicz, 1996; Ziółkowski, 2007; Krajewski *et al.*, 2011).

The Zimny Dół Valley is located in the southern part of the Kraków Upland, in the Tenczynek Horst, which borders on the Krzeszowice Graben to the south (Fig. 1). As a landform, the Zimny Dół Valley developed in the Palaeogene and was covered with loess in the Pleistocene (Gradziński, 1962; Dżułyński *et al.*, 1968). Among the typical morphological features of the Zimny Dół area are suffosion sinkholes, the walls of which are composed of loess and the bottoms of which are Upper Jurassic limestones. These sinkholes originated from the washing of the loess caprock into karst conduits that were present in the Upper Jurassic bedrock (Gradziński, 1962; Gradziński and Baryła, 2005).

The group of Upper Jurassic tors exposed in the nature preserve is characterised by numerous rectilinear passages (‘corridors’), several metres wide and with vertical rock

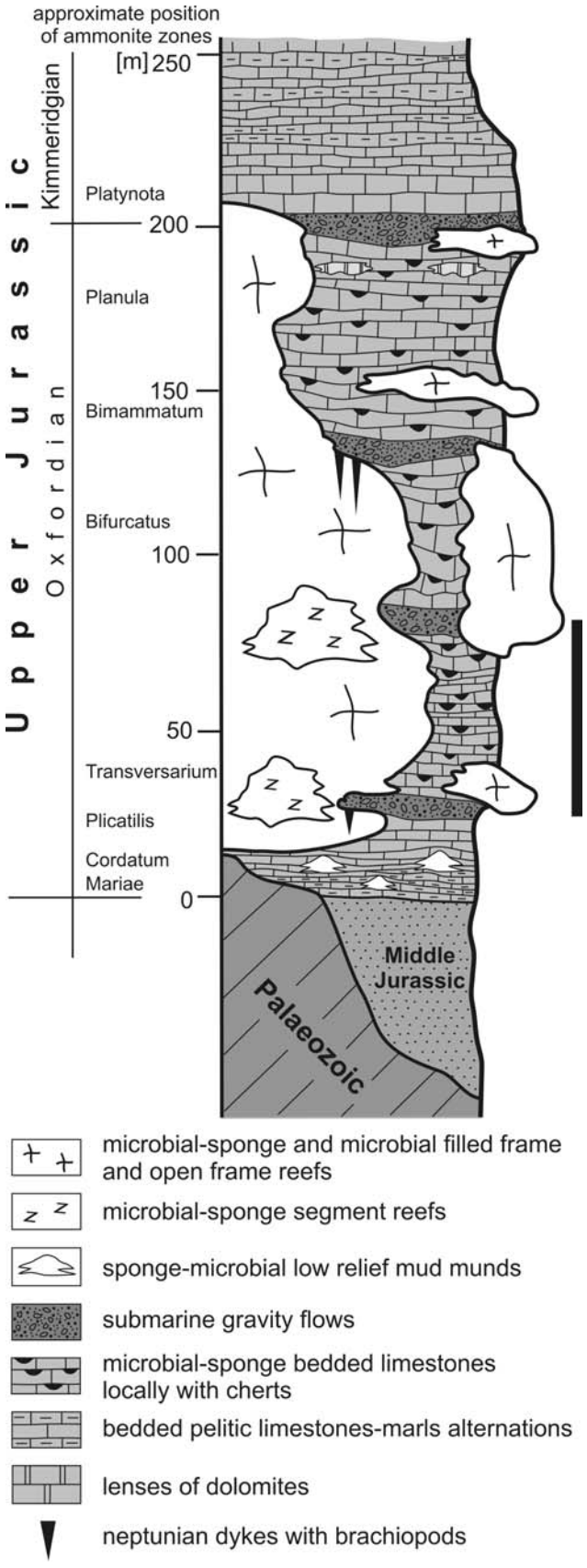

Fig. 3. Lithostratigraphic column of Upper Jurassic strata in the southern part of the Kraków–Częstochowa Upland with the approximate stratigraphic position of Upper Jurassic complex of the Zimny Dół Nature Reserve (after Matyszkiewicz *et al.* 2016; modified).

walls towering on either side (Fig. 2), formed when joint fractures were pulled apart by mass movements (Gradziński and Baryła, 2005). In the upper part of the limestone complex, one can observe particularly spectacular corridors with vertical walls, composed of pseudonodular limestones. Typical features of the tors are basal niches with overhanging 'eaves', presumably the effects of karstification of the pseudonodular limestones in conjunction with other weathering processes (Gradziński and Baryła, 2005).

The Upper Jurassic strata of the Mników area attain a maximum thickness of about 130 m, whereas those in the Zimny Dół Valley are only 50–80 m thick (Gradziński and Baryła, 2005). The exposed limestones (Fig. 3) belong to the Transversarium-Bifurcatus ammonite zones (Matyszkiewicz, 1994), corresponding to the middle/upper Oxfordian break (cf. Matyja and Wierzbowski, 2004). In the nature reserve, the Upper Jurassic limestone complex is about 40 m thick. In the eastern part of the reserve, the lower portion of the complex is dominated by a massive facies with local lenses of pseudonodular limestones.

Pseudonodular limestones dominate in the western part of the reserve, in the upper part of the stratigraphic sequence, above an elevation of 325 m a.s.l. (Fig. 2). Here, horizontal layers of pseudonodular limestones, several metres thick, rest upon massive limestones; horizons, nest-like bodies and lenses of pseudonodular limestones are enclosed within the massive facies.

TERMINOLOGY

Prior to the petrographic characterisation of the pseudonodular limestones, the terms applied to descriptions of pressure dissolution features (PDFs) must be defined, along with the terms 'nodularity' and 'pseudonodularity'.

Pressure dissolution features

PDFs result from chemical compaction, which occurs during burial diagenesis. PDFs provide important information, which can be applied to estimates of the compaction and stress histories of sedimentary basins (e.g., Pettit and Mattauer, 1995; Ebner *et al.*, 2009). All PDFs originate from the pressure solution processes that were active during burial diagenesis and/or tectonic deformation. PDF classifications are based on: (1) the presence and the degree of suturing of seam material (e.g., Weyl, 1959; Wanless, 1979; Buxton and Sibley, 1981; Railsback, 1993a, 2002); (2) the 2-D geometry of the seams and their relationships to sedimentary bedding (Park and Schot, 1968a); (3) the relative intensity of pressure solution processes (Logan and Semeniuk, 1976); (4) the relative solubility and size/shape of the adjacent rock or grain units (Trurnit, 1968a, 1968b); and (5) the amplitude and morphology of pressure dissolution within stylolites, their lateral continuity, and the thickness of the accumulated insoluble residue (Koepnick, 1984). Three basic types of PDF have been distinguished: dissolution seams, stylolites, and fitted fabrics (Wanless, 1979; Buxton and Sibley, 1981; Bathurst, 1991; Railsback, 2002).

Stylolites are serrated boundaries between two masses of rock characterised by sutured surfaces built by interpen-

etrating columns. Anisotropic structures are sometimes called 'solution cleavage' (e.g., Alvarez *et al.*, 1976, 1978; Rutter, 1983; Railsback, 1993a; Viti *et al.*, 2014). Their equivalents are so-called 'sutured seams' (Wanless, 1979). Stylolites cross-cut all fabrics, according to their composition and their degree of relative pressure solubility (cf. Trurnit, 1968a, 1968b; Logan and Semeniuk, 1976; Bathurst, 1991), cutting through all kinds of particles found in rock, namely grains, matrix and cement. Stylolites extend laterally along distances many times longer than the dimensions of single particles. However, the serrated boundaries between only two interpenetrating grains are called 'microstylolites' (cf. Koepnick, 1984; Moore, 1989). Unfortunately, this term was also used by Wanless (1979) and Marshak and Englander (1985) as a name for a dissolution seam. According to Andrews and Railsback (1997), early-forming stylolites in more heterogeneous carbonates (packstones and grainstones) are more serrated than those in late-forming stylolites in wackestones and mudstones. Stylolites may be infilled with insoluble residuum, composed mostly of clay minerals, Fe-oxides, or even organic matter.

Dissolution seams (after Bathurst, 1991) are known also by other names: solution seams (Garrison and Kennedy, 1977; Buxton and Sibley, 1981), non-sutured seams (Wanless, 1979), or wave-like stylolites (Alsharhan and Sadd, 2000). This category of PDFs is characterised by smooth, undulating boundaries between two rock masses lacking the sutured contacts typical of stylolites. Dissolution seams may occur in swarms (Bathurst, 1991) forming so-called 'flaser structures' (Garrison and Kennedy, 1977), 'horsetail structures' (Roehl, 1967) or 'wispy seams' (Alsharhan and Sadd, 2000). Dissolution seams are mostly infilled with insoluble residuum, which may lead to their misidentification as thin, marly intercalations, deposited because of a local reduction in carbonate deposition and a simultaneous increase in the supply of clay minerals. Under intense pressure solution, dissolution seams may transform limestone into marl, initially forming a so-called 'stylolaminated fabric' followed by a 'stylocumulate fabric' (cf. Logan and Semeniuk, 1976; Huber, 1987).

The third category of PDFs is fitted fabric, defined by Logan and Semeniuk (1976) as fabric where 'idens' are in contact with their neighbours along their entire margins. These idens are defined as homogeneous bodies of various sizes, which respond similarly to pressure dissolution (e.g., microbialites, sponges, bioclasts, quartz). Fitted fabrics differ from stylolites and dissolution seams in that they extend pervasively throughout a zone, affecting all idens from all sides, whereas stylolites and dissolution seams are planar features (Logan and Semeniuk, 1976; Buxton and Sibley, 1981). The boundaries between idens may be sutured or non-sutured (Buxton and Sibley, 1981; Bathurst, 1991).

All of the PDFs summarised above are discontinuity surfaces cutting through the sediment. Such surfaces may pull apart, owing to seismic tremors, weathering processes or stress relaxation. In the case of stylolites and dissolution seams, such structures are called here 'deformed stylolites' (cf. Fig. I-2 in Railsback, 2002) and 'deformed dissolution seams'. 'Deformed fitted fabrics', on the other hand, can only theoretically occur *in situ*, as any rock cut by a system of closely spaced, open fractures would readily disintegrate into weathering rubble.

Nodularity and pseudonodularity

Nodular limestones are widely described in the literature as aggregates of carbonate nodules, i.e. measured in centimetres or decimetres, comprising rounded-oval or even lenticular bodies (e.g., Kukal, 1975; Clari *et al.*, 1984; Böhm, 1992; Martire, 1996; Flügel, 2004). When such nodules form isolated lenses, which are usually separated by argillaceous seams, the term 'flaser chalk' is sometimes used (Garrison and Kennedy, 1977). The origin of nodularity in limestones has received many explanations, of which the most common are the effects of selective lithification, early cementation, dissolution, bioturbation, reworking and/or burial compaction (see e.g., Szulczewski, 1965; Bogacz *et al.*, 1968; Garrison and Fischer, 1969; Jenkyns, 1974; Tucker, 1974; Kukal, 1975; Garrison and Kennedy, 1977; Narkiewicz, 1978; Elmi, 1981; Mullinis *et al.*, 1980; Steiger and Jansa, 1984; Böhm, 1992; Martire, 1996; Łuczyński, 2001; Bertok *et al.*, 2011).

The term 'pseudonodular limestone', less frequently used in the literature, designates limestones composed of so-called 'pseudonodules' understood as 'connected nodules' (Dromart, 1989). Pseudonodules are not obvious in outcrops because of a very similar degree of coherence in both the pseudonodules and the matrix (Martire, 1996). Rocks composed of pseudonodules bear various, sometimes local names: *wapienie zrostkowe* (in Polish; Dżułyński, 1952), *ruppige Fazies* or *Flaserkalk* in German (Hummel, 1960), unlimited fitted fabric (Buxton and Sibley, 1981), oncolitic-stromatolitic facies (Massari, 1979, 1981), conglomeratic flaser chalk (Garrison and Kennedy, 1977), pseudonodular limestones (Matyszkiewicz, 1994, 1997), pseudonodular facies (Martire, 1996), or stylonodular limestones (Łuczyński, 2001). The principal, indicative feature of this facies is the presence of numerous diversified PDFs separating individual pseudonodules.

METHODOLOGY

In the Zimny Dół Nature Reserve, two rock walls were selected, in which the macroscopic facies variability of both the massive and the pseudonodular limestones was perfectly represented (sections A and B; Figs 4, 5). Both walls were accessed and sampled using rock-climbing techniques; a total of 40 samples was collected. From the two rock corridors located in the uppermost part of the Oxfordian formation (Figs 2, 6), 30 additional samples of pseudonodular limestones were taken. Finally, 25 samples were collected from other outcrops in which pseudonodular limestones occurred as lenses or nest-like bodies, embedded within the massive limestones.

From the samples collected, 80 thin sections and 35 polished sections were prepared. The principal research method was microfacies analysis and cathodoluminescence (CL) microscopy. Two thin sections, one from massive limestone and one from pseudonodular limestone, were

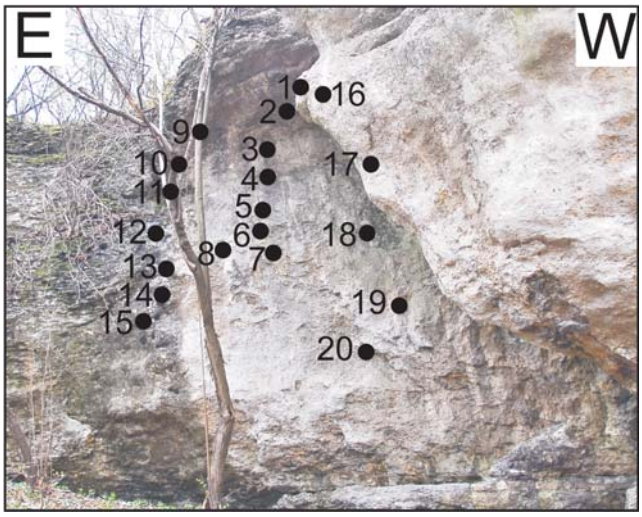

Fig. 4. Outcrop A (cf. Fig. 2). Lateral transition of massive limestone (right) into pseudonodular limestone (left). Dark spots on the outcrop wall are sampling sites.

Fig. 5. Outcrop B (cf. Fig. 2). Horizons of pseudonodular limestone in the upper, middle and lower parts of the outcrop are separated by massive limestone with a smooth weathering surface. Dark spots on the outcrop wall are sampling sites.

subjected to microprobe chemical analyses carried out along three measurement lines, perpendicular to both dissolution seams and stylolites. Finally, four polished sections, impregnated with epoxy resin were subjected to tomographic imaging at the Oil and Gas Institute, National State Research Institute, in Kraków.

PETROGRAPHIC DESCRIPTION

Outcrop A

Outcrop A is located in the middle part of the limestone formation (Figs 2, 4). Here, the authors observed the lateral contact of the pseudonodular limestones, which predominate in the eastern part of the outcrop, with the massive limestones of the smooth weathered surfaces, occurring in the western part of the exposure. Samples were collected from both the pseudonodular limestones and tight, massive limestones along two vertical and parallel sampling lines (Fig. 4).

The main fossils encountered in the pseudonodular limestone are calcified siliceous sponges, among which small (<5 mm) individuals predominate (Fig. 7A, B). Both complete specimens and rounded fragments (tuberoids) were observed. The remaining faunal assemblage is poor and includes single specimens of *Terebella lapilloides* Münster, fragments of bryozoans, plates of echinoderms (some with borings) (Fig. 7C), and fragments of thin-shelled bivalves. Secondarily important rock-forming components are microbialites (Fig. 7A) developed as peloidal, micropeloidal and agglutinating stromatolites, and also locally as clotted and layered leiolites and layered thrombolites. Microbialites occur mostly on the upper surfaces of sponges. The spaces between calcified sponges encrusted with microbialites are filled with wackestone-packstone (Fig. 7A, C), with tuberoids and rare bioclasts.

The microfacies development of both the pseudonodular and the massive limestones is very similar. Differences primarily include: (1) the greater thickness of microbialites in the massive facies; such microbialites, along with calcified siliceous sponges, built stacks of unitary sedimentary sequences (Fig. 7D; cf. Gaillard, 1983; Matyszkiewicz, 1989); (2) a lower content of fine-detrital wackestone-packstone in pseudonodular facies; and (3) the occurrence of an epifauna on the bottom surfaces of siliceous sponges, observed exclusively in the massive facies (Fig. 7D). Moreover, the massive limestones host more pores and borings, up to several millimetres across, filled with cement. In the pseudonodular limestones, all PDF categories described below were observed together with vertical gashes and subhorizontal unloading fractures (cf. Nelson, 1981), whereas in the massive facies stylolites predominate over the other PDFs and vertical gashes and unloading fractures are absent.

Outcrop B

In Outcrop B, the pseudonodular limestones (Fig. 2) form horizontal layers in the middle part of the stratigraphic sequence and occur at the base of the tor (Fig. 5). The hori-

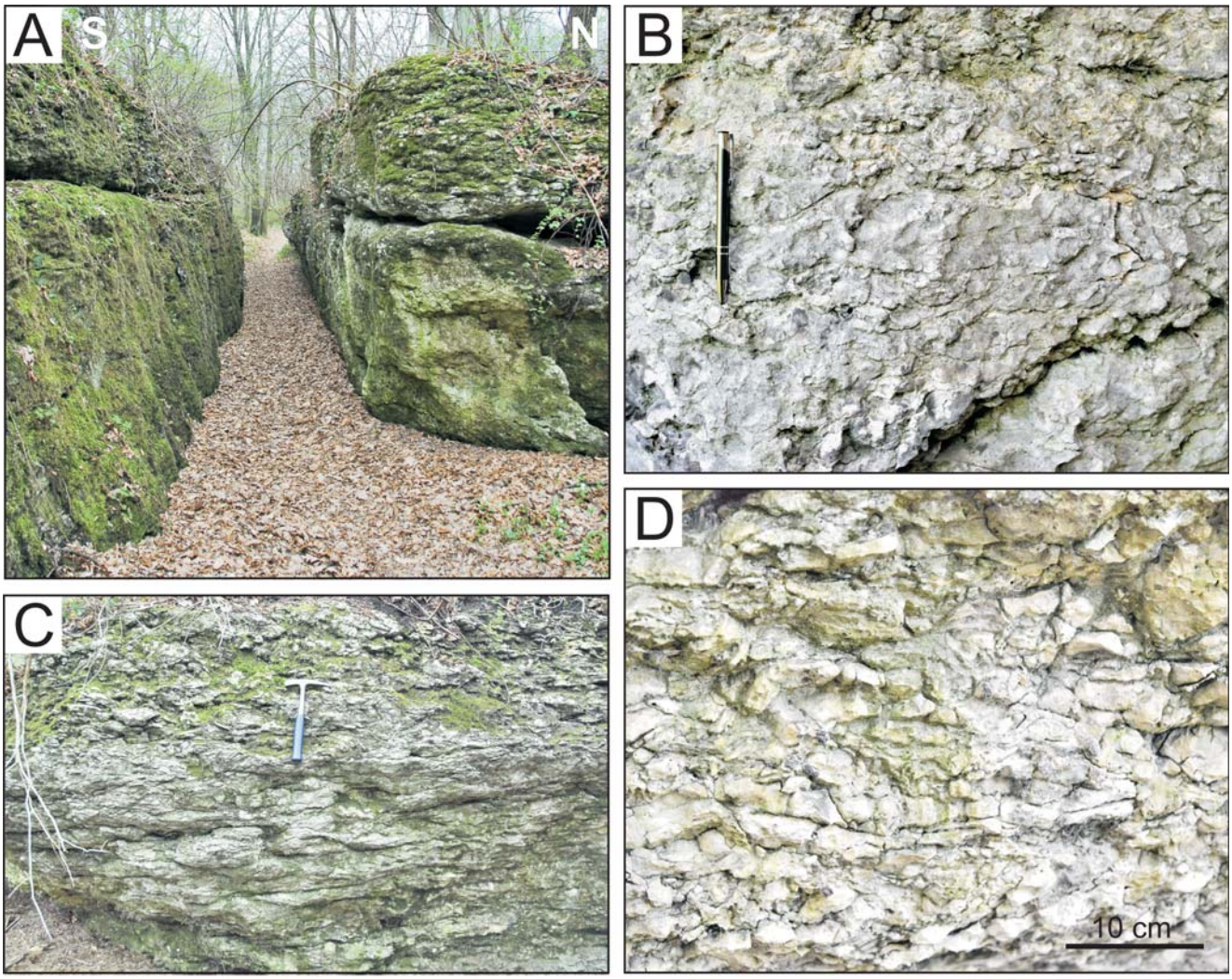

Fig. 6. Pseudonodular limestones exposed in the western corridor (cf. Fig. 2). **A**. The walls of the corridor, a W–E-trending joint fracture enlarged by mass movements, are built of pseudonodular limestone. **B**. Pseudonodular limestone, in which the boundaries between pseudonodules of various shapes and sizes are PDFs. A remarkable feature is the lack of vertical tension gashes. **C**. Surface of the southern wall of the corridor. At the bottom, the irregular, somewhat wavy, subhorizontal layers are fragments of the laminar framework. The rock in the upper part of the wall is typical pseudonodular limestone, composed of pseudonodules of various sizes and shapes. **D**. Typical pseudonodular limestone, in which boundaries between pseudonodules are PDFs and vertical/high-angle tension gashes.

zons of pseudonodular limestones are separated by tight, massive limestone with smooth outer surfaces, which grade into pseudonodular limestone in the marginal parts of the tor (Fig. 5).

In the pseudonodular limestones, the dominant components are the calcified siliceous sponge Hexactinellida observed in the life position, sometimes growing onto each other, and microbialites (Fig. 8). Most of the sponges observed are small forms, only several millimetres thick (Fig. 8B–D). Thicker (over 1 cm) sponges are less common. Microbialites grow on the upper surfaces of sponges, but their thickness does not exceed 5 mm. The bottom surfaces of these sponges are free of epifauna, unlike the Oxfordian sponges, known from both the bedded and massive limestone facies in the Kraków area (Matyszkiewicz, 1989). Microbialites are developed as layered leiolites, layered thrombolites and diversified stromatolites, i.e., micropeloidal, peloidal and agglutinating. Between sponges with overgrowing microbialites is a zone of fine-detrital wackestone-packstone, which locally hosts rounded tuberoids up to 2 mm in diameter (dominated by smaller grains). In the wackestone-packstone, laminae of layered leiolites can be observed, sometimes displaced over short distances along the vertical gashes (Fig. 8A). The remaining fossil assemblage is poor and includes single specimens of *Terebella lapilloides*, fragments of serpulids, bivalves, and echinoderms.

Both the pseudonodular and massive facies reveal similar microfacies development. The porosities of both facies are rather low. Small (about 1 mm across) caverns, usually entirely geopetally filled with granular and blocky cements and internal sediments, are observed only in the massive facies. In the pseudonodular limestones, all of the PDF categories described below are represented. Moreover, horizontal and subhorizontal PDFs are usually interconnected with vertical or high-angle gashes (Fig. 8A, D), absent from the massive facies, which is dominated by stylolites; dissolution seams are much less common.

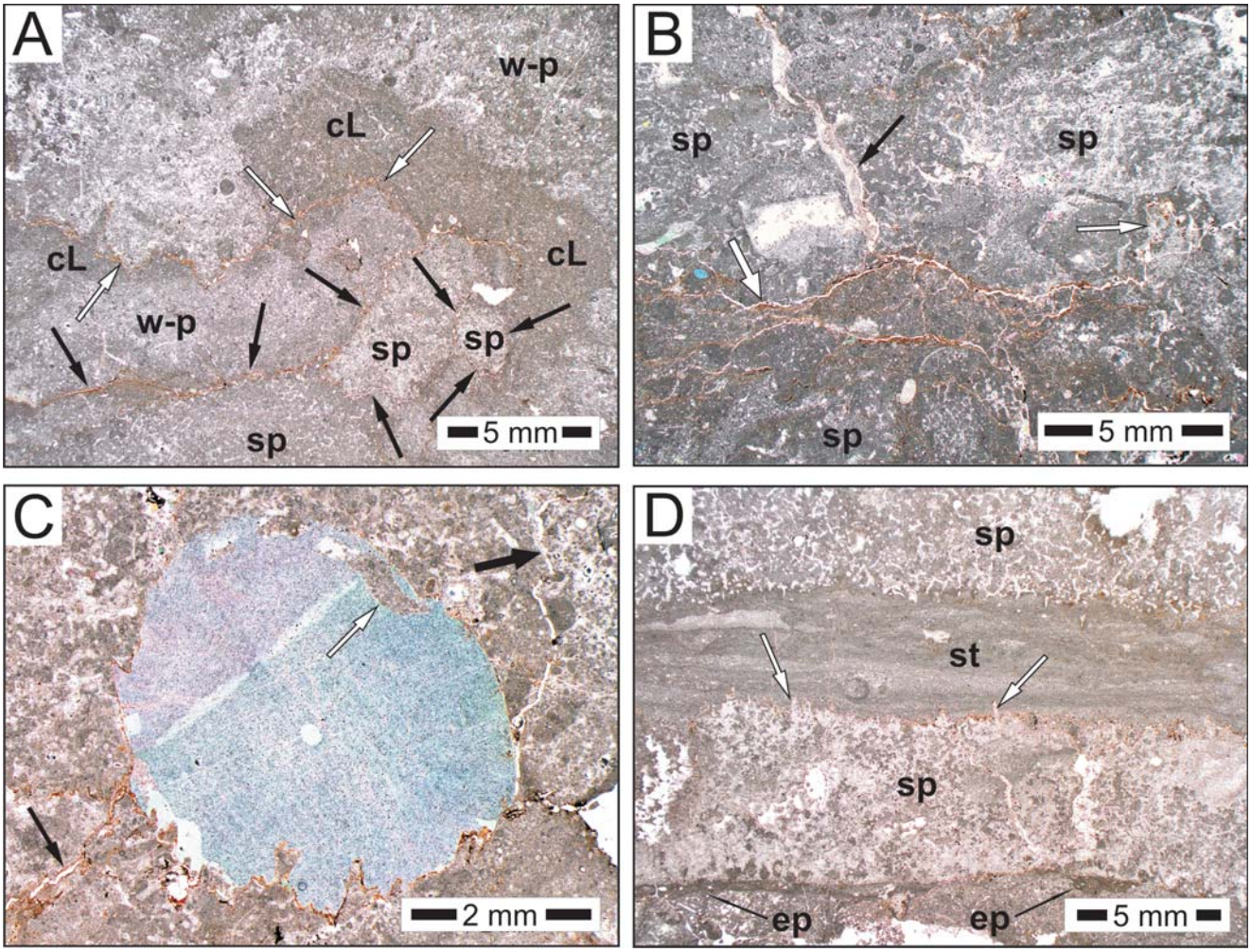

Fig. 7. Microfacies of pseudonodular (A–C) and massive (D) limestones in Outcrop A (cf. Figs 2, 4). **A**. Pseudonodules in the higher parts of the sequence. The outer surfaces of calcified siliceous sponges (sp) are bordered by stylolites (black arrows). The space between sponges is filled with fine-grained wackestone-packstone (w-p), overgrown by clotted leiolite (cL). The boundaries of the clotted leiolite only locally are given enhanced definition by stylolites (white arrows). **B**. Pseudonodules from the lower part of the sequence. Limestone with numerous sponges (sp) is cross-cut by dissolution seams, which locally branch into horsetail structures (thick white arrow). The dissolution seam changes laterally (to the right) into a high-amplitude stylolite (thin white arrow). In the upper left, a high-angle fracture, which is a deformed dissolution seam (black arrow), occurs. **C**. Pseudonodules in the lower part of the sequence. An echinoid plate with a small boring (white arrow) is seen in the centre. Apart from a small fragment in the upper part, the boundary between the echinoderm plate and the enclosing wackestone-packstone follows a stylolite, particularly evident in the lower part of the plate. Lower left: partly deformed dissolution seam (thin black arrow). Upper right: tension gash (thick black arrow). **D**. Massive facies in the middle part of the sequence. Typical unitary sedimentary sequences, composed of calcified siliceous sponges (sp) with epifauna on the bottom surface (ep) and stromatolites (st) overgrowing the upper surface. In the centre, the low-amplitude stylolite, developed on the upper surface of a sponge, is made up of only single higher-amplitude columns (white arrows).

Outcrops in the eastern and western corridors

The walls of both corridors are made up of pseudonodular limestone, in which horizontal layers, composed of wavy beds several centimetres thick and separated by interbedding planes (Figs 2, 6), were observed. Locally, such layers grade into lenses, up to 50 cm thick. Observations of polished sections impregnated with epoxy resin showed that the margins of pseudonodules follow various PDF surfaces (Fig. 9A–D) the patterns of which reflect the shapes of calcified siliceous sponges with their overgrowing microbialites. Only the pseudonodules composed of wackestone-packstone present more regular, rectilinear margins, which follow the dissolution seams and high-angle and vertical gashes (Fig. 9D).

The microfacies development of the pseudonodular limestones is similar to that of the sediments described above. Characteristic features include the presence of borings in echinoderm plates and bivalve shells, later filled with micropeloidal packstone (Fig. 10A), as well as, above all, the broken and sometimes rotated fragments of brachiopods and bivalve shells and the calcified skeletons of Hexactinellida sponges (Fig. 10B–D).

The PDFs are represented by common dissolution seams and stylolites (Figs 11, 12), locally secondarily deformed. Both the horizontal and subhorizontal PDFs are in-

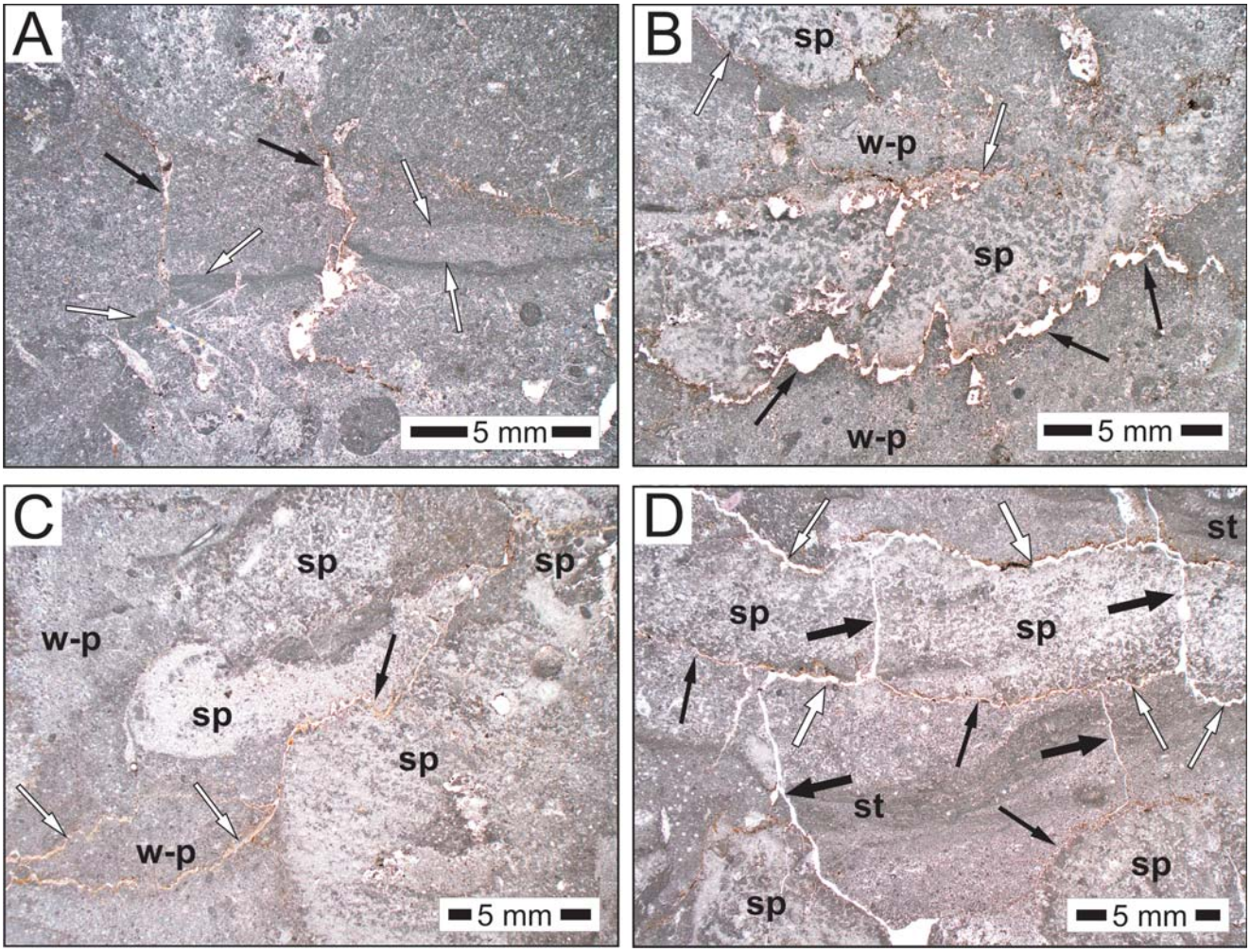

Fig. 8. Microfacies of pseudonodular limestone from Outcrop B (cf. Figs 2, 5). **A**. Wackestone-packstone with locally developed thin films of layered leiolites (white arrows). In the centre, the two vertical, partly opened fractures (black arrows) are tension gashes, along which a small displacement of sediment is documented by a shift of the layered leiolite lamina. Upper part of the sequence. **B**. A calcified siliceous sponge (sp) is in contact with wackestone-packstone (w-p) along the PDF. A deformed stylolite, developed on the bottom surface of the sponge, locally grades laterally into a deformed dissolution seam (black arrows). Stylolites and dissolution seams (white arrows) are developed on the upper surface of the lower sponge and on the lower surface of the upper sponge. Upper part of the sequence. **C**. Calcified siliceous sponges (sp), enclosed on the left in wackestone-packstone (w-p). Lower left: wackestone-packstone hosts horizontal dissolution seams (white arrows), which change their orientation to vertical on the right, at the boundary of a sponge, and then continue again as partly deformed dissolution seams and stylolites (black arrow), reflecting the shapes of sponges. Lower part of the sequence. **D**. A deformed dissolution seam (thick white arrows), deformed stylolites (thin white arrows), and stylolites (thin black arrows) developed on the outer surfaces of calcified siliceous sponges (sp) with crusts of agglutinated and peloidal stromatolites (st). The rock is cut by vertical and high-angle tension gashes (thick black arrows) at various openings, which form a network of fractures along with the PDFs, separating the pseudonodules. Lower part of the sequence.

terconnected by vertical and high-angle open fractures, which separate the limestone into fragments several centimetres in diameter.

PRESSURE DISSOLUTION FEATURES IN THE PSEUDONODULAR LIMESTONES OF THE ZIMNY DÓŁ VALLEY

In the pseudonodular limestones, the PDFs are represented by: (1) dissolution seams, (2) deformed dissolution seams, (3) stylolites, and (4) deformed stylolites. All of these PDF categories locally may grade laterally into each other.

The dissolution seams (Figs 7B, 8B, C, 9A, D, 11B, D, F, 12A, B, D, E, 13) are subplanar, non-serrated surfaces between the two rock bodies, usually arranged horizontally or subhorizontally. In most cases, dissolution seams have developed along the lower surfaces of calcified siliceous sponges or, less commonly, their upper surfaces, or at the topmost surfaces of the microbialites, overgrowing the sponges. Occasionally, dissolution seams occur also in fine-grained wackestone-packstone. If the siliceous sponges are not horizontal, dissolution seams sometimes follow their

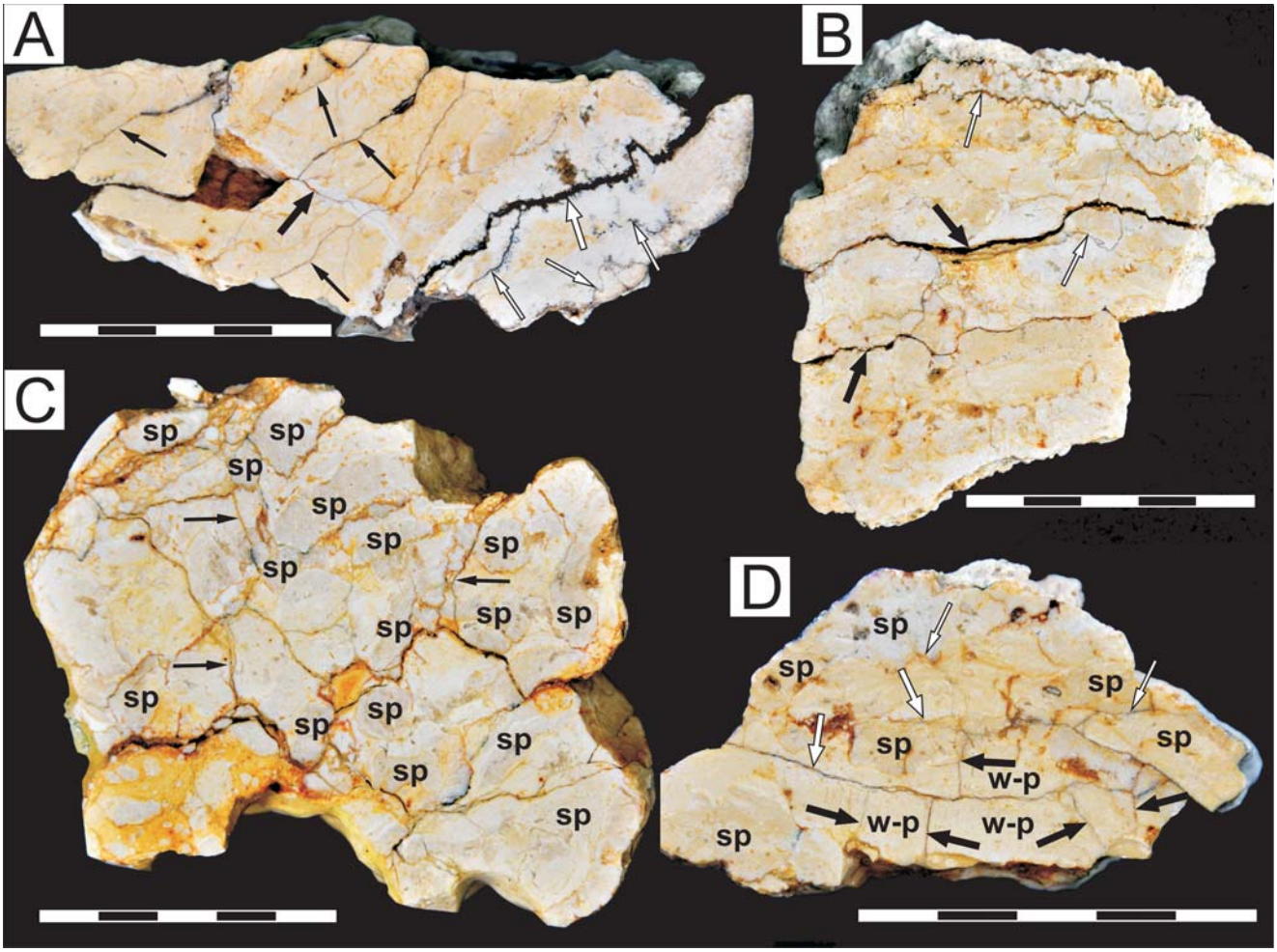

Fig. 9. Polished sections of pseudonodular limestones from the western and eastern corridors. Bar scale: 5 cm. **A**. Limestone cut by a PDF network: stylolites (thin white arrows), a deformed stylolite with surfaces covered with black Mn-oxides (thick white arrow), dissolution seams (thin black arrows), and a tension gash (thick black arrow), perpendicular to the seams. **B**. Horizontal and subhorizontal stylolites (thin white arrows) parallel to partly deformed dissolution seams (thick black arrows). **C**. Irregularly distributed pseudonodules in contact with each other mainly along various PDFs and tension gashes (black arrows). Most nodules are calcified siliceous sponges (sp), covered with crusts of microbialites. **D**. Pseudonodular limestone, composed mostly of calcified siliceous sponges (sp) and wackestone-packstone (w-p). The boundaries of the pseudonodules, composed mostly of wackestone-packstone, are dissolution seams (thick white arrows) and tension gashes (thick black arrows), and show more regular, straight-line patterns, as opposed to pseudonodules composed of sponges, the boundaries of which are stylolites (thin white arrows).

shapes and thus may slope at high angles. Locally, dissolution seams grade laterally into deformed dissolution seams or deformed stylolites. As well, fine subhorizontal branches may diverge from dissolution seams, forming incipient horsetail structures (Figs 7B, 12A). Some dissolution seams intersect the bases of interpenetrating, rectangular columns of stylolites, provided the stylolite amplitudes exceed about 1 mm (Fig. 11B, C, E, F). The widths of dissolution seams reach 0.5 mm; amplitudes are usually less than 1 mm. The boundaries of dissolution seams cutting through the pseudonodular limestones are diffuse and complicated, whereas in the massive limestones such boundaries are well-defined (Fig. 13). The dissolution seams are filled with insoluble argillaceous residuum, commonly accompanied by brownish Fe-oxides, in which rare fragments of echinoderm plates are preserved along with fine clasts of sediments more resistant to pressure dissolution (Fig. 13). Dolomite crystals were encountered sporadically along the margins of rocks, intersected by dissolution seams (Matyszkiewicz, 1994).

The deformed dissolution seams (Figs 8B–D, 11C–F, 12A, C, E, F) are non-serrated, open fractures, arranged parallel to dissolution seams. Exceptionally, high-angle or vertical deformed dissolution seams were observed, as well. These structures differ from vertical and high-angle gashes in the presence of crusts of undissolved residuum along the fracture walls. Sometimes, wackestone-packstone cut by deformed dissolution seams is darkened close to the seam walls. The amplitudes of deformed dissolution seams are similar to those of dissolution seams. Openings are usually up to several millimetres wide, but may reach maximum values up to 1 cm.

The stylolites reveal serrated surfaces, resulting from the mutual interpenetration of two rock bodies. This is the most diversified category of PDF (Figs 7, 8B–D, 9, 10B–D,

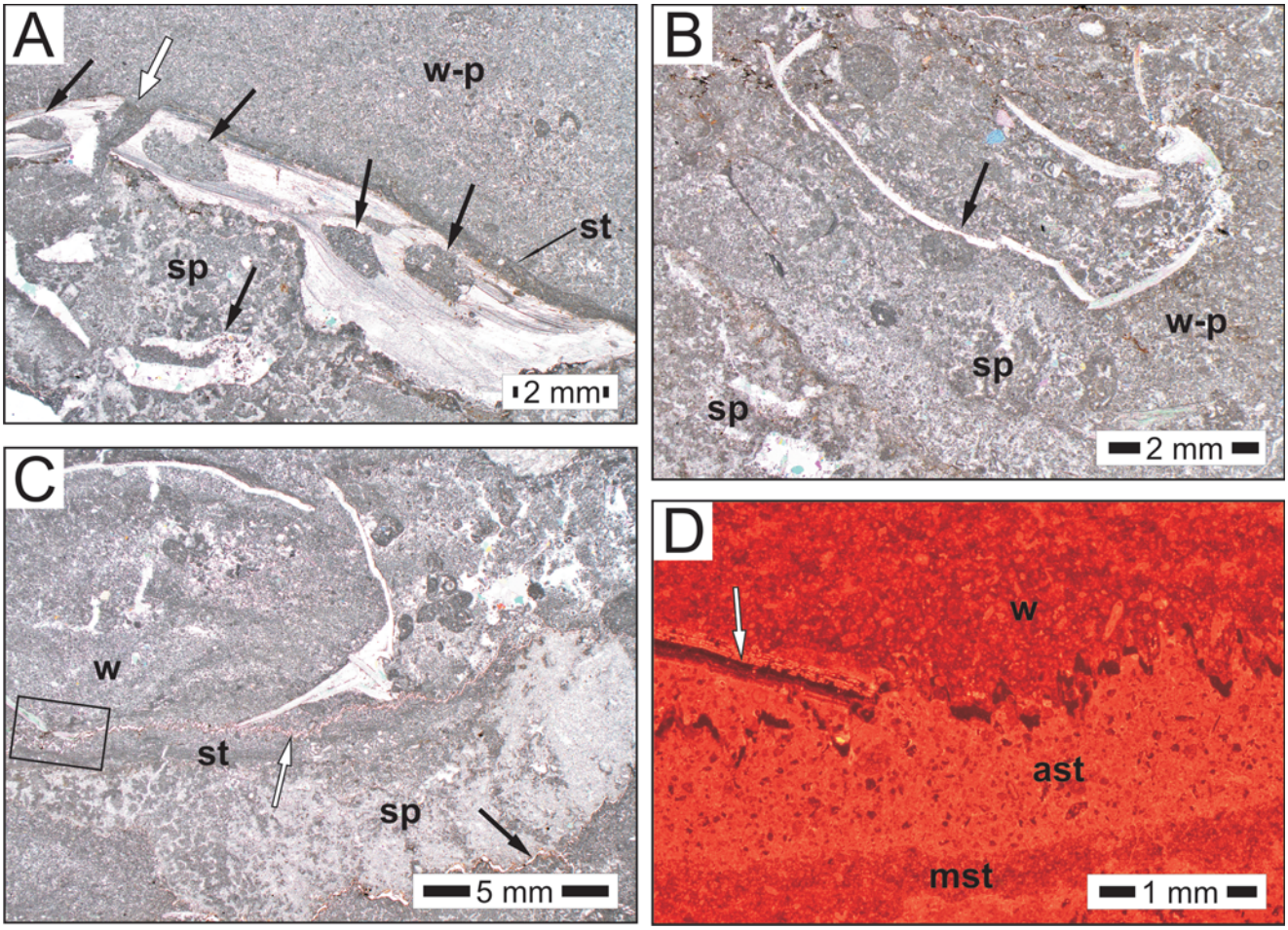

Fig. 10. Features of mechanical and chemical compaction in pseudonodular limestones. **A**. Broken (white arrow) fragment of a bivalve shell, located at the upper surface of a siliceous sponge (sp) and covered by wackestone-packstone (w-p). A layer of agglutinating stromatolite (st) covers the surface of the shell. The bivalve shell and the calcified skeleton of the sponge show borings (black arrows), filled with micropeloids and partly with cement. **B**. The broken shell of a brachiopod is embedded in wackestone-packstone (w-p) with microstylolite developed at the contact of the shell fragment with a circular tuberoid (arrow). Fragments of calcified siliceous sponges (sp) are seen in the bottom part of the wackestone-packstone. **C**. Upper left: the broken shell of a brachiopod is filled with wackestone (w) with irregular leiolite laminae. The lower part of the shell was consumed by a horizontal stylolite (white arrow), developed on the upper surface of a microbialite, overgrowing the upper surface of a siliceous sponge (sp). The lower surface of this sponge is cut by a deformed stylolite (black arrow). Insert shown in Fig. 10D. **D**. CL image of a stylolite, which consumed a fragment of a brachiopod shell. The preserved part of the shell is marked with an arrow. The interior of the shell is filled with wackestone (w). A stylolite has developed on an already lithified agglutinating stromatolite (ast), below which micropeloidal peloidal stromatolite laminae (mst) occur.

11, 12). Usually, the stylolites are horizontal or subhorizontal, but rare vertical forms were also observed. The stylolite pattern within the limestone reflects the shapes of the outer surfaces of siliceous sponges or microbialites growing on the sponges. Sometimes, stylolites characterised by a general horizontal arrangement change over to high-angle or even vertical forms over a short distance and then return again to a horizontal pattern, following the outer surfaces of flat-lying sponges (Fig. 8C). The amplitude of stylolites observed at the bottom surfaces of sponges is somewhat greater than that seen at their top surfaces. Some stylolites also cross-cut the wackestone-packstone; such forms are usually horizontal. Most observed stylolites show amplitudes of up to 2 mm, but larger (over 5 mm) and smaller (below 0.1 mm) forms also were encountered. The widths of columns vary from 0.1 to several millimetres. Usually, stylolites of greater amplitudes show wider columns. The dominant forms are conical columns, in which the amplitudes increase with the increasing widths of the bases of the columns. Occasionally, mostly in the massive facies, stylolite columns are highly elongated cuboids with diameters of about 0.1 mm or less. Some columns are cross-cut at the base by dissolution seams (Fig. 11E, F). The thickness of the infillings of sutured seams is usually less than 0.1 mm. The infilling material is insoluble residuum with brownish Fe-oxides, or Fe-oxides alone. The thickness of the residuum is similar at the slopes of stylolite columns, but usually higher at their crests. Distinct asymmetry in the thickness of insoluble residuum on the slopes of columns was observed only in a single sample (Fig. 11C). Stylolites developed on fossil fragments other than siliceous sponges either remain unfilled with insoluble residuum, or, where residuum exists, its thickness is negligible. Such stylolites are typically characterised by very small amplitudes (below 0.1 mm).

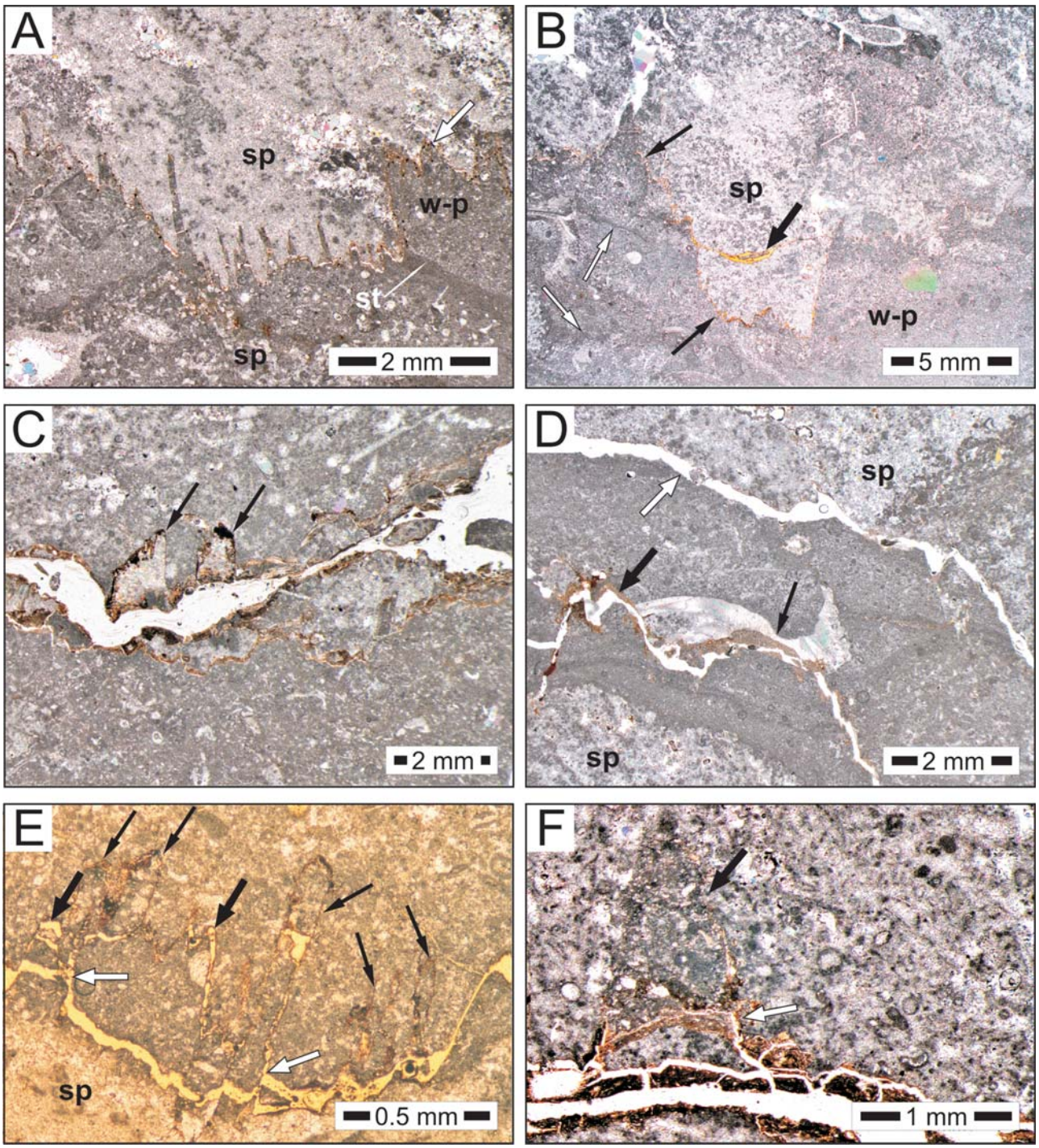

Fig. 11. PDFs from massive (A) and pseudonodular (B–F) limestones. **A**. Centre: stylolites of very narrow columns and amplitudes up to 2 mm are developed in the lower part of a calcified siliceous sponge (sp), at the contact with an adjacent siliceous sponge seen beneath. Bottom right: the preserved fragment of a stromatolite (st) is covered with wackestone-packstone (w-p), which is in contact with the upper siliceous sponge along a stylolite with wide, conical columns (arrow). **B**. Stylolites (thin black arrows) of amplitudes about 1 cm, developed at the bottom surface of a calcified siliceous sponge (sp) and wackestone-packstone (w-p) with initial microbial crusts (white arrows). One of the stylolite columns is cut at the base by a dissolution seam (thick black arrow). **C**. Deformed dissolution seam, which originated from the transformation of a stylolite with preserved fragments of the crests of stylolite columns (arrows). **D**. Upper part: an unloading fracture (white arrow), formed at the lower surface of a siliceous sponge (sp). The PDF seen in the lower part was formed on laminated microbialites, overgrowing the upper surface of another sponge, and is visible on the left as a deformed dissolution seam (thick black arrow), which grades laterally to the right into a horizontal dissolution seam with preserved insoluble residuum (thin black arrow); further to the right, it evolves into a high-angle deformed stylolite. **E**. A high-amplitude stylolite of narrow, cuboidal (thin black arrows) and wide, conical (thick black arrows) columns, developed at the surface of a siliceous sponge (sp). The stylolite columns are cut at the base of each by a deformed dissolution seam (white arrows). **F**. A dissolution seam, filled with brownish insoluble residuum and partly deformed at the bottom, replaces a stylolite. The only relic of this stylolite is a conical column (black arrow), cut at the base by a dissolution seam (white arrow).

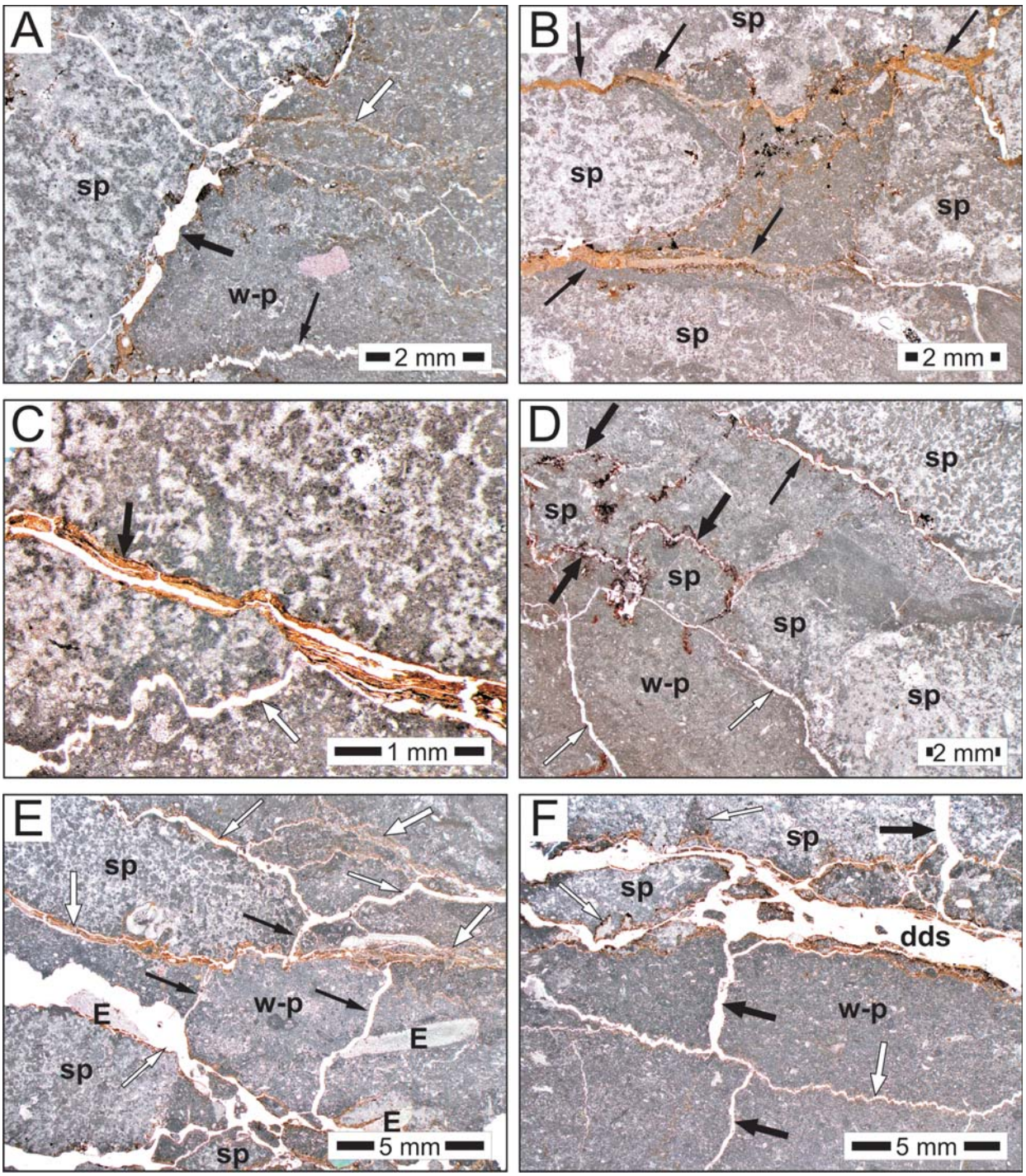

Fig. 12. Diversified PDFs in pseudonodular limestone. **A**. Contact of a siliceous sponge (sp) with wackestone-packstone (w-p), along which a deformed dissolution seam was formed (thick black arrow). In the centre of the wackestone-packstone, fine dissolution seams branch out, forming a horsetail structure (white arrow). In the lower part, wackestone-packstone is cut by horizontal low-amplitude deformed stylolites (thin black arrow). **B**. Boundstone with numerous calcified siliceous sponges (sp) is surrounded by dissolution seams, infilled with insoluble residuum (arrows). **C**. A calcified sponge cut by a deformed dissolution seam (black arrow) with preserved brownish insoluble residuum. The seam is connected to a deformed stylolite (white arrow). **D**. Limestone divided into pseudonodules by a network of various discontinuities: deformed stylolites (thin black arrow), irregularly distributed dissolution seams replacing low-amplitude stylolites (thick black arrows), and high-angle tension gashes (thin white arrows) cutting through wackestone-packstone (w-p). Most discontinuities follow the outer surfaces of siliceous sponges (sp). **E**. Readily disintegrating pseudonodular limestone cut by discontinuities: dissolution seams (thick white arrows), deformed dissolution seams (thin white arrows), and high-angle tension gashes (black arrows). Most PDFs cross-cutting the rock follow the shapes of siliceous sponges (sp). Tension gashes are arranged roughly perpendicular to PDFs and cross-cut wackestone-packstone (w-p) with frequent fragments of echinoderms (E). **F**. A regular network of discontinuities in wackestone-packstone (w-p) includes tension gashes (black arrows) and subhorizontal deformed stylolites (thick white arrow). In the upper part, a deformed dissolution seam (dds) with preserved crests of stylolites (thin white arrows) developed along the bottom surface of a siliceous sponge, which is additionally cross-cut by a tension gash.

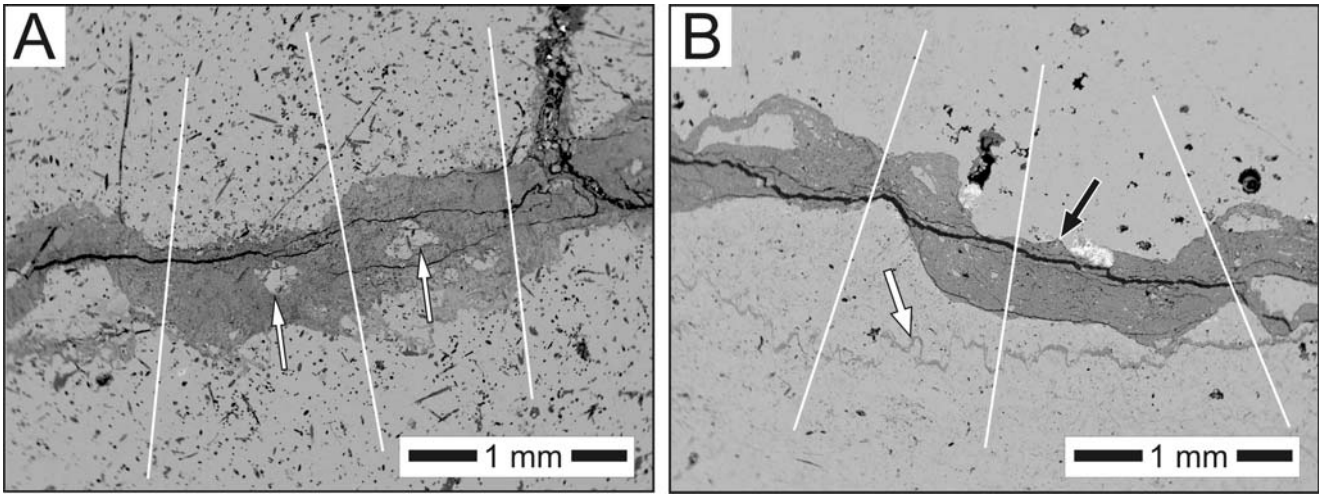

Fig. 13. BSC image of PDFs in pseudonodular (A) and massive (B) facies with lines marked along points, at which microprobe analyses were made (cf. Table 1). **A**. A dissolution seam with irregular boundaries cutting through pseudonodular limestone. Fine rock fragments seen in insoluble residuum filling the seam are relics that remained undissolved during pressure dissolution (arrows). **B**. A dissolution seam (black arrow) and stylolite (white arrow) cut through massive limestone. Like the dissolution seam dissecting pseudonodular limestone, the insoluble residuum hosts fragments of limestone, more resistant to pressure dissolution (right and left sides of dissolution seam). The boundaries of the dissolution seam are sharp.

Table 1

Results of microprobe point analyses carried out along the measurement lines marked in Figure 13

Sample			CaO	Al_2O_3	FeO	MgO	MnO	SiO_2	SrO
K	L	av.	54.370	0.446	0.090	0.393	0.030	0.962	0.051
		max.	58.856	18.584	1.401	1.342	0.143	29.235	0.427
		min.	13.066	0	0	0	0	0	0
	DS	av.	37.817	2.976	0.722	0.534	0.020	8.631	0.019
		max.	53.957	7.638	1.896	1.282	0.131	20.526	0.100
		min.	0	0.086	0.068	0.113	0	0.244	0
SG	L	av.	54.437	0.188	0.374	0.392	0.018	0.955	0.025
		mx.	58.263	6.508	10.102	0.999	0.096	24.764	0.151
		min,	24.197	0	0	0.108	0	0	0
	DS	av.	17.311	7.829	2.017	1.128	0.011	41.052	0.015
		max.	53.488	15.909	7.876	2.350	0.049	84.948	0.127
		min.	2.090	0.226	0.102	0.115	0	0.973	0
	ST	av.	20.220	6.739	7.549	1.339	0.015	30.436	0.023
		max.	29.852	8.719	19.803	2.055	0.025	36.212	0.047
		min.	7.051	3.930	0.814	0.693	0	24.500	0

Sample K is pseudonodular limestone from the western corridor (cf. Fig. 2); sample SG was collected from a massive limestone in outcrop A (cf. Fig. 2). The remarkable variability of the chemical composition of dissolution seams results from the presence of fine clasts of limestone, more resistant to pressure dissolution, within particular seams (cf. Fig. 13). L – limestone; DS – dissolution seam; ST – stylolite

The deformed stylolites (Figs 8B, D, 11D, 12A, D, F) are open, serrated fractures, arranged parallel to stylolites. Their openings may be as much as 0.5 mm wide, although narrow forms predominate. The amplitudes of deformed stylolites are apparently smaller than those of stylolites. Rock surfaces on both sides of deformed stylolites sometimes show traces of dissolution. Deformed stylolites are especially common in rocks cut by numerous, vertical or high-angle gashes.

GEOCHEMISTRY OF PDFS INFILLING

Microprobe point chemical analyses (Table 1) were carried on along measurement lines perpendicular to a dissolution seam cutting the pseudonodular limestone (Fig. 13A) and to a dissolution seam and stylolite cutting the massive limestone (Fig. 13B). The dissolution seam in the pseudonodular limestone showed clear depletion of CaO and SrO and enrichment with Al_2O_3, FeO and SiO_2 by com-

parison with the enclosing limestone. As well, an increased amount of MgO was noted, whereas the MnO content is similar to that analysed in the limestone.

Both the dissolution seam and the stylolite cutting through the massive limestone indicate enrichment in Al_2O_3, FeO, SiO_2 and MgO as well as depletion of CaO by comparison with the enclosing limestone (Table 1). The contents of MnO and SrO are similar. Some differences in chemical composition were noted between the dissolution seam and the stylolite: infilling of the latter is enriched in FeO and depleted in SiO_2 by comparison with the dissolution seam (Table 1).

STRUCTURES ASSOCIATED WITH THE PDFS

The pseudonodular limestones from the Zimny Dół Nature Reserve host high-angle or vertical, usually open fractures, i.e. so-called 'tension gashes' (cf. Nelson, 1981) (Figs 8A, D, 12D–F). Occasionally, crusts of Fe-oxides were observed at the surfaces of these fractures. The tension gashes are usually wider than deformed stylolites, but narrower than deformed dissolution seams. Rock surfaces along the tension gashes are rough, but this morphology differs from the serrated surfaces of stylolites and the wavy surfaces of dissolution seams. The tension gashes form a vertical network, connecting dissolution seams, deformed dissolution seams and deformed stylolites. However, in the parts of rock cut mostly by stylolites, tension gashes appear only sporadically.

The other structures associated with the PDFs are horizontal and subhorizontal fractures with openings up to several millimetres (Fig. 11D). These structures, which differ from deformed dissolution seams in their lack of relicts of undissolved residuum along the fracture walls, are presumably so-called 'unloading fractures' (cf. Nelson, 1981).

The network of discontinuities within the rocks studied is illustrated by the spatial imaging, generated by computer tomography (Fig. 14). The fragments of rock, in which discontinuities do not occur, are the pseudonodules.

DISCUSSION

Pseudonodular limestones *vs* other types of carbonate buildups

The Oxfordian pseudonodular limestones are specific forms of carbonate buildups called 'segment reefs' (Matyszkiewicz *et al.*, 2012, 2015b), in which sessile reef-builders are adjacent to and may be in contact with each other, but are mostly disarticulated and therefore mainly parauthochtonous (Riding, 2002). The main components of the pseudonodular limestones are Hexactinellida sponges, accompanied by microbialites and finer-grained matrix. These limestones contain rather scarce small voids, filled with carbonate cements. Sponges are arranged randomly or may accumulate in horizons, *in situ* or with minimal post-mortem displacement. By comparison with the Upper Jurassic massive limestones of the Kraków–Częstochowa Upland, the pseudonodular limestones exhibit: (1) a higher content of sponges, which are mostly small forms represented almost exclusively by Hexactinellida (cf. Trammer, 1982, 1989; Matyszkiewicz, 1997); (2) exceptionally rare occurrences of epifauna on the bottom surfaces of the sponges (cf. Matyszkiewicz, 1989); (3) distinct depletion of other fossils, which include single brachiopods, ammonites, belemnites, fragments of bivalves, single serpules, *Terebella lapilloides* and fragments of echinoderms (plates and spines of echinoids); (4) the total absence of organisms, indicating shallow carbonate depositional environments, as in the case of the Štramberk limestones (cf. Matyszkiewicz and Słomka, 2004; Kołodziej, 2015); (5) a markedly smaller proportion of microbialites (cf. Matyszkiewicz *et al.*, 2012); (6) spectacular examples of mechanical compaction effects, such as broken brachiopod shells, displaced fragments of microbialites, and calcified siliceous sponges; and, above all, (7) the presence of numerous and diversified PDFs, associated high-angle or vertical tension gashes, and subhorizontal to horizontal unloading fractures.

Fauna and sedimentation rate

One of the important features of pseudonodular limestones in the Zimny Dół Nature Reserve is an unusual abundance of hexactinellid siliceous sponges and, simultaneously, an insignificant number of lithistid sponges. Recent hexactinellids are opportunistic organisms, typical of environments characterised by very low water energy and a water temperature of below 15 °C (Mackie *et al.*, 1983). Siliceous sponges are common in sediments of the lower part of Upper Jurassic succession of the southern part of the Kraków–Częstochowa Upland. These fossils were described from marls and from carbonate buildups of the low-relief carbonate mud mound type and from space cluster reefs (Trammer, 1982; 1985; Matyszkiewicz *et al.*, 2015b). In the lowermost part of the Upper Jurassic succession, Lithistida sponges predominate; they are replaced further up the sequence by hexactinellids (Trammer, 1982, 1989). In carbonate buildups developed as agglutinated microbial reefs and open frame reefs, siliceous sponges are much less common and locally can even be absent (Matyszkiewicz *et al.*, 2012).

Unlike other Oxfordian facies containing siliceous sponges in the Kraków area, the pseudonodular limestones apparently are dominated by small hexactinellids of thickness around several millimetres, as previously noted by Dżułyński (1952). This seems to be related to the diversified feeding modes of sponges. Lithistids are filter feeders living on bacteria, which are most abundant in the upper part of water columns, whereas the structure of osmotrophic hexactinellids enables them to consume colloidal organic matter or dissolved organic carbon (Krautter, 1998). These nutrients are confirmed by the remaining benthic fauna assemblage, in which low-diversity filter-feeding organisms (e.g., brachiopods) are scarce. If the supply of these nutrients is poor, hexactinellids tend to reduce their wall thickness, which improves their contact with sea water; or in the case of morphovariable taxa, they expand their surfaces by developing thin, plate- or dish-shaped forms (Krautter, 1998).

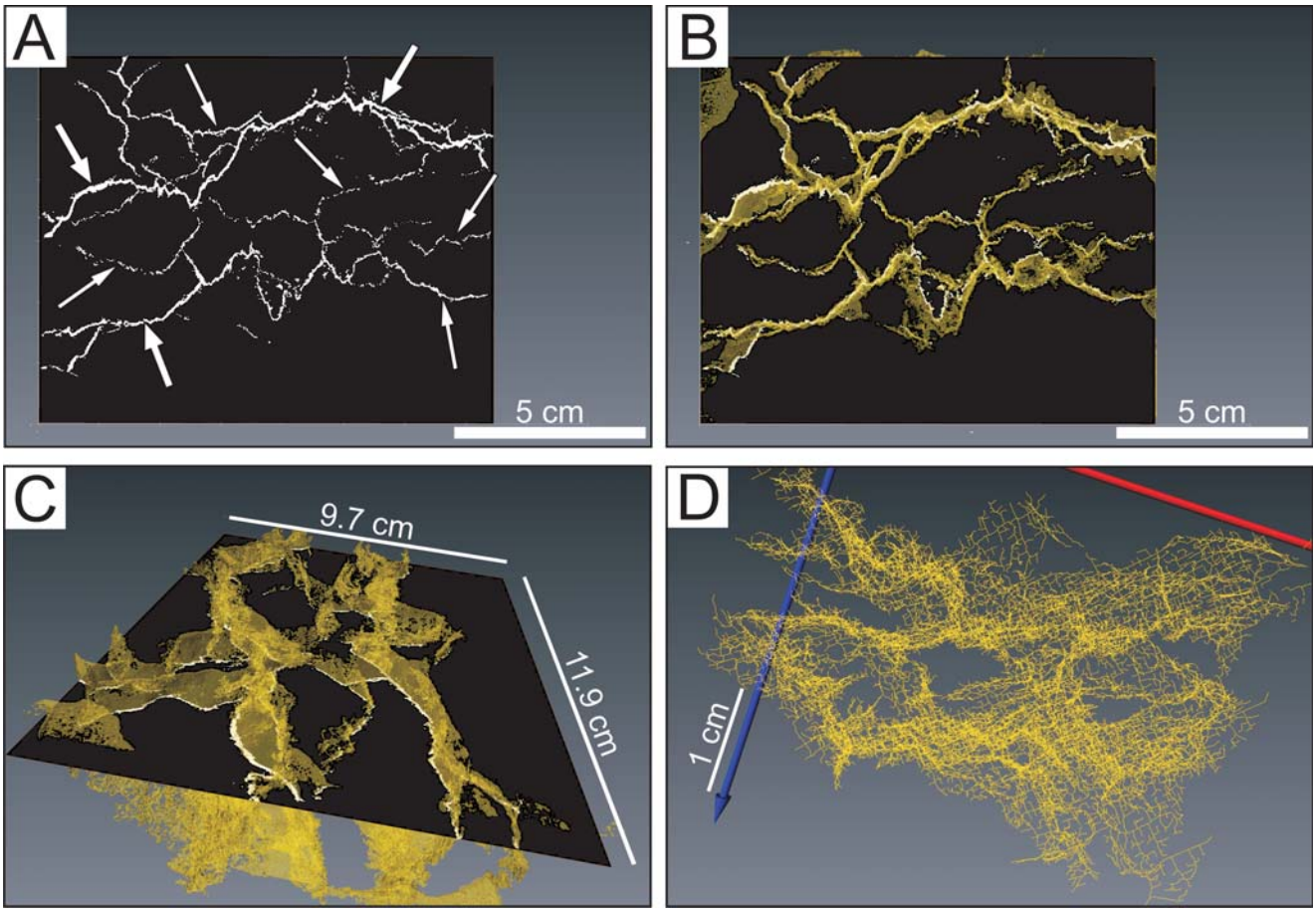

Fig. 14. A polished section of pseudonodular limestone (A) and its spatial tomographic images (B-D). **A**. a network of discontinuities within pseudonodular limestone, displayed using the tomographic method. Discontinuities are stylolites (thin white arrows) and dissolution seams (thick white arrows). **B**. A spatial tomographic image of PDFs in pseudonodular limestone, oriented as in A, with PDFs propagating from the surface towards the interior of the limestone sample. **C**. A spatial tomographic image of the pseudonodular limestone surface, illustrated in Figure A and B, obtained by rotation 90° to the left and slight tilting of the surface of the section to the right. **D**. An image of a discontinuity network in pseudonodular limestone, built of PDFs, tension gashes and unloading fractures, obtained by assigning lines of equal width to all types of discontinuity. The fields between yellow lines are pseudonodules.

Given a nutrient supply, which has been reduced to moderate, sponges develop thin, plate-shaped morphotypes. With a low nutrient supply, they are replaced by microbialites (Matyszkiewicz *et al.*, 2012). Contrastingly, in conditions of elevated sediment input, sponge populations are represented by smaller and less-diversified individuals (Krautter, 1998). Hexactinellid sponges with dictyid architecture are unknown on soft grounds (Tabachnick, 1991; Krautter, 1998). However, increasing sedimentation rates greatly reduce or even prevent the growth of an epifauna on the bottom surfaces of sponges, a feature typical of the fauna of pseudonodular limestones. On the other hand, when other groups of benthic fauna appear (e.g. echinoderm plates, bivalve shells), they occasionally show traces of borings, which document episodes of lower deposition rates.

The Upper Jurassic fine-grained pseudonodular limestones of the western subalpine basin were interpreted by Dromart (1989) as the products of: (1) slow currents, which winnowed the micrite from the upper surface of lime beds, producing incipient wavy bedding and leaving the clay that was more cohesive and resistant to resuspension; and (2) bioturbation, which incorporated argillaceous sediments from the over- and underlying layers. These processes operated with low sedimentation rates. Similarly, Martire (1996) interpreted the origin of pseudonodular limestones from the Rosso Ammonitico Veronese as being the result of pulsating currents, which enabled micrite accumulation and were followed by long and repeated phases of cementation, bioturbation, and current reworking. These processes were controlled by regional-scale changes of depositional environments in sedimentary basins.

The pseudonodular limestones in the Zimny Dół Valley show no traces of the impact of bottom currents. Moreover, bioturbation is rare in these limestones. It seems that the pseudonodular limestones were deposited in a low-energy environment, in which the dominantly moderate sedimentation rates and moderate nutrient availability were subject to periodic fluctuations (Matyszkiewicz *et al.*, 2012) documented by the development of siliceous sponges.

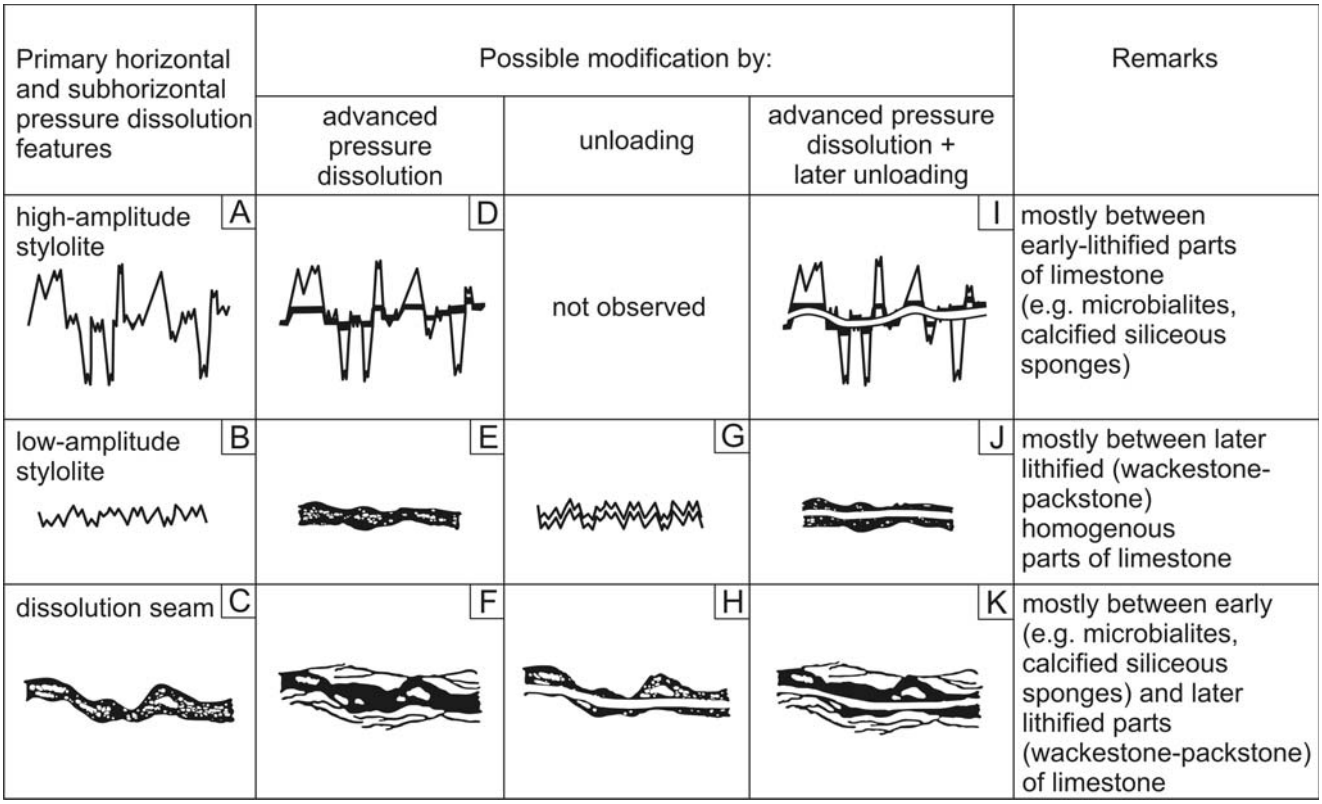

Fig. 15. Types of primary PDFs in pseudonodular limestones and their possible transformations, caused by pressure dissolution during the second stage of chemical compaction or by relaxation of the rock, or both. Primary PDFs (A–C) were generated during the first stage of chemical compaction, i.e. in the Late Jurassic. After Early Cretaceous deposition pause and partial erosion of Upper Jurassic sediments, causing a decline in overburden load, pressure dissolution locally restarted, owing to the deposition of the Upper Cretaceous formation. Hence:(1) in stylolites composed of both low- and high-amplitude segments, dissolution proceeded at the bases of interpenetrating high-amplitude stylolite columns, with the simultaneous transformation of low-amplitude stylolite segments into dissolution seams (D) ; (2) low-amplitude stylolites were entirely transformed into dissolution seams (E); (3) in dissolution seams, relics of sediment more resistant to pressure dissolution were finally dissolved and, simultaneously, horsetail structures (F) originated around these seams; (4) primary low-amplitude stylolites and dissolution seams, which remained untransformed during the second stage of chemical compaction, may have opened under the near-surface conditions as a result of stress relaxation and may have generated unloading fractures (G–H). In the high-amplitude stylolites, the strong interlocking of rock fragments precluded their opening. Unloading fractures may also have formed through the opening of PDFs, transformed in the second stage of chemical compaction (I–K).

Microbialites

In the pseudonodular limestones, microbialites typically grew on sponges and were developed as pure and layered leiolites, clotted thrombolites, and micropeloidal, peloidal, and agglutinating stromatolites (Matyszkiewicz *et al.*, 2012). Similar microbialites are observed in the massive limestones, but their abundance and thickness (particularly of stromatolites) are significantly greater.

The macroscopic textural differences between the massive and the pseudonodular facies have resulted mostly from the differing patterns of development of the rigid framework. In the massive facies, the growth of microbial-sponge associations, along with an increased proportion of microbialites, resulted in the formation of a reticulate rigid framework (Matyszkiewicz *et al.*, 2015b; cf. Pratt, 1982). However, in the pseudonodular facies, conditions favourable for the development of a rigid framework alternated with unfavourable ones, under which the microbial-sponge associations declined and were replaced by deposition of fine-detrital wackestone-packstone. Already lithified horizons built of siliceous sponges with overgrowing thin crusts of microbialites generated the horizontal, initial rigid framework (so-called ‘laminar rigid framework’; cf. Pratt, 1982) only locally, whereas the enclosing, fine-detrital wackestone-packstone remained unlithified for a relatively long time and was susceptible to mechanical compaction.

Mechanical compaction

Features of mechanical compaction are observed only in the parts of pseudonodular limestones developed as wackestone-packstone, filling the space between siliceous sponges overgrown by microbialites (Fig. 10A–D). Mechanical compaction is manifested by the broken shells of brachiopods and spines of echinoids and by fragments of siliceous sponges. These features indicate that the wackestone-packstone, unlike the siliceous sponges and the microbialites, long remained unlithified. Mechanical compaction not only broke down the rigid components of the sediment (e.g. brachiopod shells), but also led to vertical displacements of the sediment in the order of several millimetres,

usually accompanied by some rotation of the more lithified fragments embedded in the fine-detrital wackestone-packstone (cf. Braithwaite, 1989).

The results of experimental studies of the fine-detrital Oxfordian limestones of the southern part of the Kraków–Częstochowa Upland demonstrate that the peak of mechanical compaction corresponds to a burial depth of about 2 m. Below this depth, mechanical compaction decreases exponentially (Kochman and Matyszkiewicz, 2013).

Chemical compaction

The minimum burial depth of carbonate sediments, at which pressure dissolution commences, ranges from 30 (Railsback, 1993b) or 90 (Tada and Siever, 1989) to over 1,000 m (Neugebauer, 1974). The burial depth of the protolith of the Oxfordian pseudonodular limestones of the Zimny Dół Valley is difficult to estimate. However, by analogy with the Upper Jurassic sediments in the northern part of the Kraków–Częstochowa Upland, it has been suggested that the maximum burial depth of the pseudonodular limestones studied was about 500 m (Matyszkiewicz, 1999).

The timing of PDF formation is still controversial. Several authors have accepted a pre- (Park and Schot, 1968a, 1968b) or post-indurational (Manten, 1968) origin, or both (Wanless, 1979; Buxton and Sibley, 1981; Shinn and Robbin, 1983). Garrison and Kennedy (1977) proposed that the flaser structure of the Upper Cretaceous chalks of southern England predated stylolite formation and resulted from the interaction of compaction, dissolution, and partial selective lithification. Undoubtedly, the pseudonodular limestones studied underwent pressure dissolution after lithification, but the sites particularly predisposed to the development of such structures were boundaries between the components of sediment lithified both earlier (microbialites and calcified siliceous sponges) and later (wackestone-packstone). The transformations of PDFs, particularly the dissolution at the bases of stylolite columns (Fig. 11E, F), indicate that pressure dissolution proceeded in two stages, separated by a distinct break. The first stage took place at the end of the Late Jurassic, when the thickness of overburden had become sufficient to trigger the process (Kutek, 1994). The second stage developed in the Late Cretaceous, when deposition began again, following Early Cretaceous erosion (Oszczypko, 2006). The accumulation of sediments and resulting overburden load led to an increase in pressure, which triggered further chemical compaction of Upper Jurassic strata (Fig. 15).

Pressure dissolution processes are controlled by many factors, e.g., stress orientation, protolith mineralogy, fluid chemistry and temperature (cf. Logan and Semeniuk, 1976; Railsback, 1993a; Koehn *et al.*, 2007; Ebner *et al.*, 2010; Viti *et al.*, 2014). The dominant horizontal and subhorizontal arrangement of the PDFs in the pseudonodular limestones clearly demonstrates that these structures originated from overburden load. An important role in PDF formation was played by the presence in the initial sediment of phyllosilicates, which acted as catalysts in the pressure solution processes (cf. Hickman and Evans, 1995; Niemeijer and Spiers, 2005; Aharonov and Katsman, 2009; Viti *et al.*, 2014). Aharonov and Katsman (2009) state that rocks with somewhat higher contents of clay minerals are especially susceptible to dissolution and thus will accumulate more residual clays, further enhancing subsequent pressure dissolution. The lesser numbers of microbialites observed in pseudonodular limestones by comparison with the massive facies presumably resulted from somewhat higher contents of phyllosilicates, caused by a locally increased supply of fine-detrital material (including clays) from the upper parts of the carbonate buildups. This material hampered the development of microbialites (cf. Schmid, 1996; Matyszkiewicz *et al.*, 2012). Slightly higher clay contents in the protolith, from which pseudonodular limestones formed, resulted in a greater intensity of pressure dissolution in the pseudonodular limestones than in the massive limestones with lower clay content.

It seems that at the first stage of chemical compaction, pressure dissolution conditions were stable and lateral stress was absent. This is documented – since insoluble residuum is a measure of local dissolution – by the similar thicknesses of insoluble residuum on the sides of stylolite columns (cf. Railsback, 2002), in conjunction with the significantly greater thicknesses of this residuum on the crests of columns.

The dissolution seams observed in the pseudonodular limestones studied were formed during both the initial and advanced stages of chemical compaction, with the latter including the transformation of the stylolites (Fig. 15). The renewed intensity of pressure dissolution in the vicinity of dissolution seams, formed at the initial compaction stage, presumably gave rise to the development of horsetail structures (Figs 9B, 12A). The preserved fragments of the crests of stylolite columns, seen at the margins of limestone cut by dissolution seams (Fig. 11C, E, F), indicate that these structures originated from the transformation of stylolites. Stylolites with columns several millimetres high were not transformed entirely into dissolution seams (Fig. 15). Sometimes only the low-amplitude segments of a stylolite were transformed, whereas single, cuboidal columns, 0.1–0.2 mm wide (Fig. 10E), or even conical columns up to 1 mm wide at the bases (Fig. 11F) and showing amplitudes of several millimetres, were cross-cut at their bases by dissolution seams (Fig. 15).

The important components of insoluble residuum are Fe-minerals. According to Cox and Etheridge (1989), these minerals behaved passively during pressure dissolution and tended to accumulate as residual phases. However, during burial compaction, transformation of pyrite into Fe-oxides/hydroxides was possible, and even the precipitation of authigenic magnetite might have occurred (Evans and Elmore, 2006). Undoubtedly, the PDFs provided open fluid conduits during burial (Brathwaite, 1989), as indicated by increased Mg contents in the insoluble residuum and occasional precipitation of dolomite crystals at the margins of the PDFs (Matyszkiewicz, 1994).

The formation of high-angle and vertical tension gashes may have been initiated by the same stress field, which controlled the origin of the PDFs (cf. Nelson, 1981). Their opening took place under the same extensional regime as the opening of some PDFs. Both the low amplitudes and geometry of dissolution seams facilitated their opening. In contrast, only low-amplitude stylolites of simple geometry

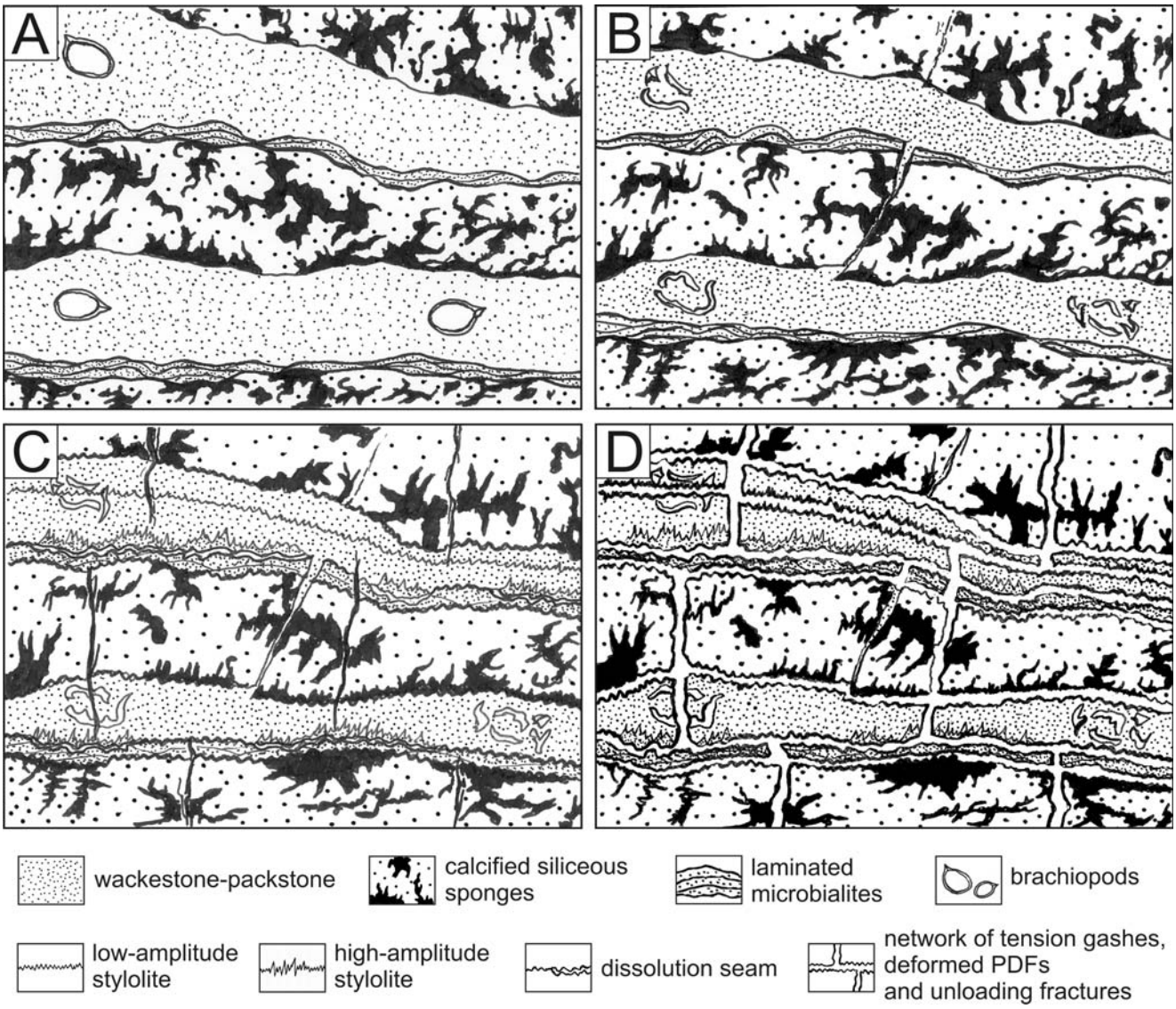

Fig. 16. Model of formation of pseudonodular limestone. **A**. Sedimentation stage (middle Oxfordian). **B**. Mechanical compaction stage (middle–late Oxfordian). **C**. Pressure dissolution stages (Late Jurassic and Late Cretaceous). **D**. Extension and stress relaxation stage (Cenozoic). The longest edge of drawings A–D is about 5 cm. Drawing by P. Kłapyta.

could be opened, whereas high-amplitude stylolites ensured strong interlocking of the rock fragments involved.

The horizontal and subhorizontal unloading fractures were most likely the effects of relaxation of the rock parallel to maximum stress direction and were related to weathering and erosion of the exposed pseudonodular limestones (cf. Nelson, 1981). Both processes emphasised the discontinuities reflected in the stylolites and dissolution seams and caused the opening of some of these structures (Fig. 15).

PROPOSED SCENARIO

The pseudonodular limestones represent segment reefs, built in a low-energy environment with a moderate sedimentation rate and moderate nutrient availability. The initial, laminar, rigid microbial-sponge framework was subjected to early lithification. This framework and fragments of it were primarily were associated with unconsolidated, fine-detrital wackestone-packstone that later was the focus of mechanical compaction (Fig. 16A). This not only increased the density of the wackestone-packstone, but also crushed and locally displaced embedded rigid fragments, e.g. shell fragments or even parts of the laminar, rigid microbial-sponge framework (Fig. 16B).

The recently observed pseudonodular texture is chiefly the result of chemical compaction, which triggered pressure dissolution processes at the end of the Late Jurassic, when the overburden load had become sufficiently high. At the margins of the already lithified components of the sediment (e.g., calcified siliceous sponges, microbialites), primarily high-amplitude stylolites were formed, whereas at the boundaries between the earlier- and later-lithified wackestone-packstone, dissolution seams were generated. In homogeneous wackestone-packstone, low-amplitude stylolites originated locally (Fig. 16C).

At the end of the Late Cretaceous, after some reduction in overburden pressure, caused by Early Cretaceous erosion (Kutek, 1994; Oszczypko, 2006), pressure dissolution processes started again, once a sufficient thickness of Upper Cretaceous sediments had been deposited. As a result, some mostly low-amplitude stylolites were transformed into dissolution seams, whereas among stylolites of diverse amplitudes, only low-amplitude segments evolved into dissolution seams, which simultaneously cross-cut the bases of interpenetrating high-amplitude columns. The propagation of pressure dissolution around the dissolution seams, formed during the initial stage of chemical compaction, led to the formation of horsetail structures. Presumably, the same stress field, which initiated pressure dissolution, gave rise to the propagation of both vertical and high-angle incipient tension gashes, which remained closed at the beginning of the process (cf. Nelson, 1981).

In the Cenozoic, under the extensional regime resulting from the overthrusting of Carpathian nappes, the tension gashes opened, along with high-angle and vertical stylolites and dissolution seams of similar patterns. Some of these tension gashes, stylolites, and dissolution seams may have become the transfer pathways for mineralising solutions that circulated within the rock formations (cf. Gołębiowska *et al.*, 2010; Matyszkiewicz *et al.*, 2015a; 2016). Under conditions of subsequent exposure, both subhorizontal and horizontal unloading fractures developed in the limestones (cf. Nelson, 1981), partly as a result of the opening of dissolution seams and stylolites of similar orientations. These processes generated a network of vertical and horizontal discontinuities, which divided the limestone into pseudonodules of various shapes and sizes (Fig. 16D). The open spaces between the rock fragments then served as conduits for karst waters.

CONCLUSIONS

1. The texture of the pseudonodular limestones resulted from two stages of chemical compaction in the Late Jurassic and Late Cretaceous.

2. During the Late Jurassic stage, high-amplitude and low-amplitude stylolites and dissolution seams were formed. The sites favourable for the development of high-amplitude stylolites were the boundaries between already lithified fragments of the laminar, rigid microbial-sponge framework. The low-amplitude stylolites formed mainly in wackestone-packstone, which was lithified somewhat later; hence, the dissolution seams originated at the contacts between the rigid microbial-sponge framework and the wackestone-packstone.

3. Late Cretaceous sedimentation enabled the renewal of pressure dissolution. A part of low-amplitude stylolites evolved into dissolution seams. In stylolites composed of both low- and high-amplitude segments, dissolution proceeded at the bases of interpenetrating high-amplitude stylolite columns, with the simultaneous transformation of low-amplitude stylolite segments into dissolution seams. The seams, which formed at the Late Jurassic stage of chemical compaction, were subjected in turn to further pressure dissolution, giving rise to the formation of horsetail structures.

4. The vertical stress field, which triggered the pressure dissolution processes, presumably resulted in the formation of high-angle and vertical incipient tension gashes, which at the beginning of the processes remained closed. In the Cenozoic, under the extensional regime generated by overthrusting Carpathian flysch nappes, the tension gashes opened up. Under the same conditions some high-angle and vertical dissolution seams and low-amplitude stylolites opened up as well, forming deformed dissolution seams and deformed stylolites.

5. During the exposure period, unloading fractures developed, due partly to the opening of some subhorizontal and horizontal dissolution seams and stylolites. The unloading fractures, along with the already existing vertical and high-angle tension gashes, formed the network, shaping the limestone into pseudonodules of various shapes and sizes.

Acknowledgements

We benefited greatly from the perceptive and constructive comments and suggestions of L. B. Railsback, L. Martire and an anonymous reviewer. The authors would like to thank M. Dohnalik for tomographic analyses. The project was funded by the National Science Centre on the basis of Contract No. DEC-2011/03/B/ST10/06327 and by a Statutory Grant from the AGH University of Science and Technology.

REFERENCES

Aharonov, E. & Katsman, R., 2009. Interaction between pressure solution and clays in stylolite development: Insights from modelling. *American Journal of Science*, 309: 607–632.

Alsharhan, A. S. & Sadd, J. L., 2000. Stylolites in Lower Cretaceous carbonate reservoirs, U.A.E. *Society for Sedimentary Geology, Special Publication*, 69: 185–207.

Alvarez, W., Engelder, T. & Lowrie, W., 1976. Formation of spaced cleavage and folds in brittle limestone by dissolution. *Geology*, 4: 698–701.

Alvarez, W., Engelder, T. & Geiser, P. E., 1978. Classification of solution cleavage in pelagic limestones. *Geology*, 6: 263–266.

Andrews, L. M. & Railsback, L. B., 1997. Controls on stylolite development: morphologic, lithologic, and temporal evidence from bedding-parallel and transverse stylolites from the US Appalachians. *Journal of Geology*, 105: 59–73.

Bathurst, R. G. C., 1991. Pressure-dissolution and limestone bedding: the influence of stratified cementation. In: Einsele, G., Ricken, W. & Seilacher, A. (eds), *Cycles and Events in Stratigraphy*. Springer, Berlin, pp. 450–463.

Bertok, C., Martire, L., Perotti, E., d'Atri, A. & Piana, F., 2011. Middle–Late Jurassic syndepostional tectonics recorded in the Ligurian Briançonnais succession (Marguareis–Mongioie area, Ligurian Alps, NW Italy). *Swiss Journal of Geosciences*, 104: 237–255.

Bogacz, K., Dżułyński, S., Gradziński, R. & Kostecka, A., 1968. Origin of crumpled limestones in the Middle Triassic of Poland. *Rocznik Polskiego Towarzystwa Geologicznego*, 38: 385–394. [In Polish, with English summary.]

Böhm, F., 1992. Mikrofazies und Ablagerungsmilieu des Lias und Dogger der Nordöstlichen Kalkalpen. *Erlanger Geologische Abhandlungen*, 121: 57–217.

Braithwaite, C. J. R., 1989. Stylolites as open fluid conduits. *Marine and Petroleum Geology*, 6: 93–96.

Buxton, T. M. & Sibley, D. F., 1981. Pressure solution features in a shallow buried limestone. *Journal of Sedimentary Petrology*, 51: 19–26.

Clari, P. A. & Martire, L., 1996. Interplay of cementation, mechanical compaction, and chemical compaction in nodular limestones of the Rosso Ammonitico Veronese (Middle–Upper Jurassic, northeasters Italy). *Journal of Sedimentary Research*, 66: 447–458.

Clari, P. A., Martini, P., Pastorini, M. & Pavia, G., 1984. Il Rosso Ammonitico Inferiore (Baiociano–Calloviano) nei Monti Lessini Settentrionali. *Rivista Italiana di Paleontologia e Stratigrafia*, 90: 15–86.

Cox, S. F. & Etheridge, M. A., 1989. Coupled grain-scale dilatancy and mass transfer during deformation at high fluid pressures: examples from Mount Lyell, Tasmania. *Journal of Structural Geology*, 11: 147–162.

Dromart, G., 1989. Deposition of Upper Jurassic fine-grained limestones in the Western Subalpine Basin. *Palaeogeography, Palaeoclimatology, Palaeoecology*, 69: 23–43.

Dżułyński, S., 1952. The origin of the Upper Jurassic limestones in the Cracow area. *Rocznik Polskiego Towarzystwa Geologicznego*, 21: 125–180. [In Polish, with English summary.]

Dżułyński, S., Krysowska-Iwaszkiewicz, M., Oszast, J. & Starkel, L., 1968. On Lower Quaternary gravels in the Sandomierz Basin. *Studia Geomorphologica Carpatho-Balcanica*, 2: 63–75. [In Polish, with English summary.]

Ebner, M., Koehn, D., Toussaint, R. & Renard, F., 2009. The influence of rock heterogeneity on the scaling properties of simulated and natural stylolites. *Journal of Structural Geology*, 31: 72–82.

Ebner, M., Piazolo, S., Renard, F. & Koehn, D., 2010. Stylolite interfaces and surrounding matrix material: Nature and role of heterogeneities in roughness and microstructural development. *Journal of Structural Geology*, 32: 1070–1084.

Elmi, S., 1981. Classifications typologique et génétique des Ammonitico Rosso et des facies noduleux ou grumeleux: essai de synthése. In: Farinacci, A. & Elmi, S. (eds), *Proceedings of the Rosso Ammonitico Symposium*. Tecnoscienza, Roma, pp. 233–249.

Evans, M. A. & Elmore, R. D., 2006. Fluid control of localized mineral domains in limestone pressure solution structures. *Journal of Structural Geology*, 28: 284–301.

Flügel, E., 2004. *Microfacies of Carbonate Rocks, Analysis, Interpretation and Application*. Springer, Berlin, Heidelberg, New York, 976 pp.

Gaillard, C., 1983. Les biohermes á spongiaires et leur environment dans l'Oxfordian du Jura méridional. *Documents des Laboratoires de Géologie de la Faculté des Sciences de Lyon*, 90: 1–515.

Garrison, R. E. & Fischer, A. G., 1969. Deep-water limestones and radiolarites of the Alpine Jurassic. In: Friedman, G. M. (ed.), *Depositional environments in carbonate rocks. Society of Economic Paleontologists and Mineralogists, Special Publications*, 14: 20–56.

Garrison, R. E. & Kennedy, W. J., 1977. Origin of solution seams and flaser structure in Upper Cretaceous chalks of Southern England. *Sedimentary Geology*, 19: 107–137.

Gołębiowska, B., Pieczka, A., Rzepa, G., Matyszkiewicz, J. & Krajewski, M., 2010. Iodargyrite from Zalas (Cracow area, Poland) as an indicator of Oligocene–Miocene aridity in Central Europe. *Palaeogeography, Palaeoclimatology, Palaeoecology*, 296: 130–137.

Gradziński, R., 1962. Origin and development of subterranean karts in southern part of the Cracow Upland. *Rocznik Polskiego Towarzystwa Geologicznego*, 31: 429–492. [In Polish, with English summary.]

Gradziński, R., 1972. *Przewodnik geologiczny po okolicach Krakowa.* Wydawnictwa Geologiczne, Warszawa, 335 pp. [In Polish.]

Gradziński, R., 2009. *Geological Map of Krakow Region without Quaternary and Terrestrial Tertiary Deposits*. Wydawnictwo Instytutu Nauk Geologicznych PAN, Kraków.

Gradziński, R. & Baryła, J., 1986. *Projekt utworzenia, zabezpieczenia i zagospodarowania rezerwatu przyrody nieożywionej „Zimny Dół" z uwzględnieniem aspektów szaty roślinnej.* Unpublished. Archiwum Zarządu Zespołu Jurajskich Parków Krajobrazowych w Krakowie, Kraków, 36 pp. [In Polish.]

Gradziński, R. & Baryła, J., 2005. Values of the Zimny Dół valley and the local nature reserve. In: Partyka, J. (ed.), *Zróżnicowanie i przemiany środowiska przyrodniczo-kulturowego Wyżyny Krakowsko-Częstochowskiej*, *Volume 3 – Supplement*. Ojcowski Park Narodowy, Ojców, pp. 11–18. [In Polish, with English summary.]

Gradziński, R. & Musielewicz-Jasińska, Z., 1992. Rezerwat przyrody nieożywionej „Zimny Dół". *Chrońmy Przyrodę Ojczystą*, 48(5): 78–83. [In Polish.]

Hickman, S. H. & Evans, B., 1995. Kinetics of pressure solution at halite-silica interfaces and intergranular clay films. *Journal of the Geological Society of London*, 148: 549–560.

Huber, S., 1987. Drucklösungserscheinungen in Karbonaten des Oxford 1 und Kimmeridge 1 der Bohrung TB-3 Saulgau (Oberschwaben). *Facies*, 17: 109–120.

Hummel, P., 1960. Petrographie, Gliederung und Diagenese der Kalke im Oberen Weissen Jura der Schwäbischen Alp. *Arbeiten aus dem Geologisch-Paläontologischen Institut der Universität Stuttgart*, 26: 1–86.

Jenkyns, H. C., 1974. Origin of red nodular limestones (Ammonitico Rosso, Knollenkalke) in the Mediterranean Jurassic: a diagenetic model. In: Hsü, K. J. & Jenkyns, H. C. (eds), *Pelagic Sediments: on Land and Under the Sea, Special Publication of the IAS, Volume 1*. Wiley-Blackwell, Oxford, pp. 249–271.

Kochman, A. & Matyszkiewicz, J., 2013. Experimental method for estimation of compaction in the Oxfordian bedded limestones of the southern Kraków-Częstochowa Upland, Southern Poland. *Acta Geologica Polonica*, 63: 681–696.

Koehn, D., Renard, F., Toussaint, R. & Passchier, C. W., 2007. Growth of stylolite teeth patterns depends on normal stress and finite compaction. *Earth and Planetary Science Letters*, 257: 582–595.

Koepnick, R. B., 1984. Distribution and vertical permeability of stylolites within a Lower Cretaceous carbonate reservoir, Abu Dhabi, United Arab Emirates. In: Moussly, M., Bathurst, R. G. C. & El-Ouri, A. (eds), *Stylolites and Associated Phenomena Relevance to Hydrocarbon Reservoirs. Special Publication of the Abu Dhabi National Reservoir Research Foundation*. U.A.E. Foundation, Abu Dhabi, pp. 261–278.

Kołodziej, B., 2015. Geological context and age of the Štramberk-type limestones from the Polish Outer Carpathians: an overview. *Neues Jahrbuch für Geologie und Paläontologie, Abhandlungen*, 276: 173–179.

Krajewski, M., Matyszkiewicz, J., Król, K. & Olszewska, B., 2011. Facies of the Upper Jurassic–Lower Cretaceous deposits from the southern part of the Carpathian Foredeep basement in the Kraków–Rzeszów area (southern Poland). *Annales Societatis Geologorum Poloniae*, 81: 269–290.

Krautter, M., 1998. Ecology of siliceous sponges: application to the environmental interpretation of the Upper Jurassic sponge facies (Oxfordian) from Spain. *Cuadernos de Geología Ibérico*, 24: 223–239.

Kukal, Z., 1975. On the origin of nodular limestones. *Časopis pro Mineralogii a Geologii*, 20: 359–367.

Kutek, J., 1994. Jurassic tectonic events in south-eastern cratonic Poland. *Acta Geologica Polonica*, 44: 167–221.

Logan, B. W. & Semeniuk, V., 1976. Dynamic metamorphism process and products in Devonian carbonate rocks, Canning basin, western Australia. *Geological Society of Australia*, *Special Publication*, 6: 1–138.

Łuczyński, P., 2001. Pressure-solution and chemical compaction of condensed Middle Jurassic deposits, High-Tatric series, Tatra Mountains. *Geologica Carpathica*, 52: 91–102.

Mackie, G. O., Lawn, I. D. & Pavans de Ceccatty, M., 1983. Studies on hexactinellid sponges II. Excitability, conduction and coordination of responses in *Rhabdocalyptus dawsoni* (Lambe, 1873). *Philosophical Transactions of the Royal Society*, B301: 401–418.

Manten, A. A., 1968. Pre- or post-induration formation of stylolite seams; a reply. *Geologie en Mijnbouw*, 47: 114–115.

Marok, A. & Reolid, M., 2012. Lower Jurassic sediments from the Rhar Roubane Mountains (Western Algeria): Stratigraphic precisions and synsedimentary block-faulting. *Journal of African Earth Sciences*, 76: 50–65.

Marshak, S. & Engelder, T., 1985. Development of cleavage in limestones of a fold-thrust belt in eastern New York. *Journal of Structural Geology*, 7: 345–35.

Martire, L., 1996. Stratigraphy, facies and synsedimentary tectonics in the Jurassic Rosso Ammonitico Veronese (Altopiano di Asiago, NE Italy). *Facies*, 35: 209–236.

Massari, F., 1979. Oncoliti e stromatoliti pelagiche nel Rosso Ammonitico Veneto. *Memorie Società Geologica Italiana*, 32: 1–21.

Massari, F., 1981. Cryptalgal fabrics in the Rosso Ammonitico sequences of the Venetian Alps. In: Farinacci, A. & Elmi, S. (eds), *Rosso Ammonitico Symposium Proceedings.* Edizioni Tecnoscienza, Roma, pp. 435–469.

Matyja, B. A. & Wierzbowski, A., 2004. Stratigraphy and facies development in the Upper Jurassic of the Kraków-Częstochowa Upland and the Wieluń Upland. In: Partyka, J. (ed.), *Zróżnicowanie i przemiany środowiska przyrodniczo-kulturowego Wyżyny Krakowsko-Częstochowskiej*, *Volume 1 – Nature*. Ojcowski Park Narodowy, Ojców, pp. 13–18. [In Polish, with English summary.]

Matyszkiewicz, J., 1989. Sedimentation and diagenesis of the Upper Oxfordian cyanobacterial–sponge limestones in Piekary near Kraków. *Annales Societatis Geologorum Poloniae*, 59: 201–232.

Matyszkiewicz, J., 1994. Remarks on the deposition of pseudonodular limestones in the Cracow area (Oxfordian, southern Poland). *Berliner Geowissenschaftliche Abhandlungen*, E13: 419–439.

Matyszkiewicz, J., 1996. The significance of *Saccocoma*–calciturbidites for the analysis of the Polish Epicontinental Late Jurassic Basin: an example from the Southern Cracow-Wieluń Upland (Poland). *Facies*, 34: 23–40.

Matyszkiewicz, J., 1997. Microfacies, sedimentation and some aspects of diagenesis of Upper Jurassic sediments from the elevated part of the Northern peri-Tethyan Shelf: a comparative study on the Lochen area (Schwäbische Alb) and the Cracow area (Cracow-Wieluń Upland, Poland). *Berliner Geowissenschaftliche Abhandlungen*, E21: 1–111.

Matyszkiewicz, J., 1999. Sea-bottom relief versus differential compaction in ancient platform carbonates: a critical reassessment of an example from Upper Jurassic of the Cracow-Wieluń Upland. *Annales Societatis Geologorum Poloniae*, 69: 63–79.

Matyszkiewicz, J., Felisiak, I., Hoffman, M., Kochman, A., Kołodziej, B., Krajewski, M. & Olchowy, P., 2015b. Transgressive Callovian succession and Oxfordian microbial-sponge carbonate buildups in the Kraków Upland. In: Haczewski, G. (ed.), *Guidebook for Field Trips Accompanying 31st IAS Meeting of Sedimentology Held in Kraków on 22nd–25th of June 2015.* Polish Geological Society, Kraków, pp. 51–73.

Matyszkiewicz, J., Kochman, A. & Duś, A., 2012. Influence of local sedimentary conditions on development of microbialites in the Oxfordian carbonate buildups from the southern part of the Kraków-Częstochowa Upland (South Poland). *Sedimentary Geology*, 263–264: 109–132.

Matyszkiewicz, J., Kochman, A., Rzepa, G., Gołębiowska, B., Krajewski, M., Gaidzik, K. & Żaba, J., 2015a. Epigenetic silicification of the Upper Oxfordian limestones in the Sokole Góry (Kraków-Częstochowa Upland); relation to facies development and tectonics. *Acta Geologica Polonica*, 65: 181–203.

Matyszkiewicz, J., Krajewski, M., Kochman, A., Kozłowski, A. & Duliński, M., 2016. Oxfordian neptunian dykes with brachiopods from the southern part of the Kraków-Częstochowa Upland (Southern Poland) and their links to hydrothermal vents. *Facies*, 62. DOI: 10.1007/s10347-016-0464-x

Matyszkiewicz, J. & Słomka, T., 2004. Reef-microencrusters association *Lithocodium aggregatum – Bacinella irregularis* from the Cieszyn limestones (Tithonian–Berriasian) of the Outher Western Carpathians (Poland). *Geologica Carpathica*, 55: 449–456.

Moore, C. H., 1989. *Carbonate Diagenesis and Porosity*. Elsevier, New York, 338 pp.

Mullins, H. T., Neumann, A. C., Wilber, R. J. & Boardman, M. R., 1980. Nodular carbonate sediment on Bahamian slopes; possible precursors to nodular limestones. *Journal of Sedimentary Petrology,* 50: 117–131.

Narkiewicz, M., 1978. Genesis of nodular structure in Upper Devonian limestones, Olkusz–Zawiercie area. *Kwartalnik Geologiczny*, 22: 693–706. [In Polish, with English summary].

Nelson, R. A., 1981. Significance of fracture sets associated and classification. *American Association of Petroleum Geologists Bulletin*, 67: 313–322.

Neugebauer, J., 1974. Some aspects of cementation in chalk. In: Hsü, K. J. & Jenkyns, H. C. (eds), *Pelagic Sediments: on Land and under the Sea, Special Publication of the IAS, Volume 1*. Wiley-Blackwell, Oxford, pp. 149–176.

Niemeijer, A. & Spiers, C.-J., 2005. Influence of phyllosilicates on fault strength in the brittle–ductile transition: insights from rock Insight from rock analogue experiments. In: Bruhn, D. & Burlini, L. (eds), *High-strain zones: Structure and physical properties. Geological Society of London Special Publication*, 245: 303–327.

Oszczypko, N., 2006. Late Jurassic–Miocene evolution of the Outer Carpathian fold-and thrust belt and its foredeep basin (Western Carpathians, Poland). *Geological Quarterly*, 50: 169–194.

Park, W. C. & Schot, E. H., 1968a. Stylolites: their nature and origin. *Journal of Sedimentary Petrology*, 38: 175–191.

Park, W. C. & Schot, E. H., 1968b. Stylolitization in carbonate rocks. In: Müller, G. & Friedman, G. M. (eds), *Recent Developments in Carbonate Sedimentology in Central Europe*. Springer, Berlin, pp. 66–74.

Pettit, J. P. & Mattauer, M., 1995. Paleostress superimposition deduced from mesoscale structures in limestone – the Matelles exposure, Languedoc, France. *Journal of Structural Geology*, 17: 245–256.

Pratt, B. R., 1982. Stromatolitic framework of carbonate mud-

mounds. *Journal of Sedimentary Petrology*, 52: 1203–1227.

Railsback, L. B., 1993a. Contrasting styles of chemical compaction in the Upper Pennsylvanian Dennis Formation in the Midcontinent region, USA. *Journal of Sedimentary Petrology*, 63: 61–72.

Railsback, L. B., 1993b. Intergranular pressure dissolution and compaction in a Plio–Pleistocene grainstone buried no more than 30 meters: Shoofly oolite, southwestern Idaho. *Carbonates and Evaporites*, 8: 163–169.

Railsback, L. B., 2002. *An Atlas of Pressure Dissolution Features*. Department of Geology of the University of Georgia. http://www.gly.uga.edu/railsback /PDFindex1.html

Riding, R., 2002. Structure and composition of organic reefs and carbonate mud mounds: concepts and categories. *Earth–Science Reviews*, 58: 163–231.

Roehl, P. O., 1967. Stone Mountain (Ordovician) and Interlake (Silurian), facies analogs of recent low-energy marine and subaerial carbonates, Bahamas. *American Association of Petroleum Geologists Bulletin*, 51: 1979–2032.

Rutter, E. H., 1983. Pressure solution in nature, theory, and experiment: *Journal of the Geological Society*, 140: 725–740.

Schmid, D. U., 1996. Marine Mikrobolithe und Mikroinkrustierer aus dem Jura. *Profil*, 9: 101–251.

Shinn, E. A. & Robbin, D. M., 1983. Mechanical and chemical compaction in fine-grained shallow-water limestones. *Journal of Sedimentary Petrology*, 53: 595–618.

Steiger, T. & Jansa, L. F., 1984. Jurassic limestones of the seaward edge of the Mazagan Carbonate Platform (NW African continental margin, Morocco). In: Hinz, K., Winterer, E. L., *et al.* (eds), *Initial Reports, Deep Sea Drilling Project*, 79: 449–491.

Szulczewski, M., 1965. Observation sur la genese des calcaires noduleux des Tatras. *Rocznik Polskiego Towarzystwa Geologicznego*, 35: 243–261. [In Polish, with French summary.]

Tabachnick, K. R., 1991. Adaptation of the *Hexactinellid* sponges to deep-sea life. In: Reitner, J. & Keupp, H. (eds), *Fossil and Recent Sponges*. Springer, Berlin, pp. 378–386.

Tada, R. & Siever, R., 1989, Pressure solution during diagenesis: *Annual Reviews Earth and Planetary Sciences*, 17: 89–118.

Trammer, J., 1982. Lower to Middle Oxfordian sponges of the Polish Jura. *Acta Geologica Polonica*, 32: 1–39.

Trammer, J., 1989. Middle to Upper Oxfordian sponges of the Polish Jura. *Acta Geologica Polonica*, 39: 49–91.

Trurnit, P., 1968a. Pressure solution phenomena in detrital rocks: *Sedimentary Geology*, 2: 89–114.

Trurnit, P., 1968b. Analysis of pressure solution contacts and classification of pressure solution phenomena. In: Müller, G. & Friedman, G. M. (eds), *Recent Developments in Carbonate Sedimentology in Central Europe*. Springer, Berlin, pp. 75–84.

Tucker, M., 1974. Sedimentology of Palaeozoic pelagic limestones: the Devonian Griotte (Southern France) and Cephalopodenkalk (Germany). In: Hsü, K. J. & Jenkyns, H. C. (eds), *Pelagic Sediments: on Land and under the Sea, Special Publication of the IAS, Volume 1*. Wiley-Blackwell, Oxford, pp. 71–92.

Viti, C., Collettini, C. & Tesei, T., 2014. Pressure solution seams in carbonatic fault rocks: Mineralogy, micro/nanostructures and deformation mechanism. *Contributions to Mineralogy and Petrology*, 167: 1–15.

Wanless, H. R., 1979. Limestone response to stress: pressure solution and dolomitization. *Journal of Sedimentary Petrology*, 49: 437–462.

Weyl, P. K., 1959. Pressure solution and the force of crystallization: a phenomenological theory. *Journal Geophysical Research*, 64: 2001–2025.

Ziółkowski, P., 2007. Stratygrafia i zróżnicowanie facjalne górnej jury wschodniej części Wyżyny Krakowskiej. *Volumina Jurassica*, 4: 25–38. [In Polish.]